A review of the physical properties of base metal mattes

by A.W. Sundström*, J.J. Eksteen*, and G.A. Georgalli*

Synopsis

This paper reviews the development and suitability of various important thermophysical and electrical properties with respect to base metal mattes. Areas of focus include the critical validation of measurements of viscosity, density, surface and interfacial tension, electrical conductivity, and an overview of the various experimental methods used to determine these properties. Accurate physical property data of mattes are critical in process modelling and computational fluid dynamic modelling of smelting and converting operations employed in the extraction of copper, nickel, cobalt and platinum group metals.

Introduction

An important prerequisite to the design of pyrometallurgical processing equipment used in the extraction of copper, nickel, cobalt and platinum group metals from base metal sulphide concentrates is an understanding of the physical properties and behaviour of molten matte. These properties are often used incorrectly as a result of the scarcity and difficulty in obtaining reliable data.

This paper investigates the physical properties (viscosity, density, surface and interfacial tension, and electrical conductivity) of molten mattes in pyrometallurgical processes and may be used as a guide for selecting suitable matte properties. The paper is structured to introduce the experimental methods used by various authors and then to elaborate on and compare the results of their work pertaining to a specific physical property.

The data reviewed in this paper should be useful in the process modelling or computational fluid dynamic (CFD) modelling of matte smelting and converting operations.

Viscosity

An understanding of the sensitivity of viscosity with regard to temperature and composition in any liquid system is a key property in mass transfer occurrences. In pyrometallurgical processes much attention has been paid to slag viscosity, with alloy and matte viscosities receiving much less attention.

Experimental method

Due to the difficulty in locating viscosity data of mattes, only two methods of measurement are mentioned. The Meyer-Schvidkovskii method, as described by Nikiforov *et al.*[1], makes use of a high-temperature vacuum viscosity meter and equations for low-viscosity liquids[2]. Pure metals were fused with elementary sulphur to obtain pure compounds of Ni_3S_2, FeS, CoS, and Cu_2S. Binary alloy systems of these compounds were formed by fusing the initial sulphides under vacuum. Nikiforov *et al.*[1] reported a relative error of 10% for the determination of the temperature dependence of viscosity when using this method.

Dobrovinskii *et al.*[3] determined the viscosity of quasi-binary mixtures of FeS, Co_4S_3, and Ni_3S_2 in a viscometer that measured viscosity from the logarithmic decrease of damping vibrations from a corundum crucible that contained the sample and was suspended in a heating furnace. Each test was performed in an atmosphere of helium (high purity). The measurement error did not exceed 10% when the apparatus was calibrated with pure metals of known viscosity such as Sn, Ni, Co and Cu.

Viscosity-temperature-composition relationships

The temperature dependence of the dynamic viscosity of the pure compounds Ni_3S_2, FeS, and Cu_2S[1] can be seen in Figure 1, with the viscosity of all of these components being read off on the left axis. In order to put these values into perspective, the viscosity of pig iron (Fe-C,

* *Department of Process Engineering, University of Stellenbosch, Matieland, South Africa.*

 SA ISSN 0038–223X/3.00 + 0.00. Paper received May 2007; revised paper received May 2008.

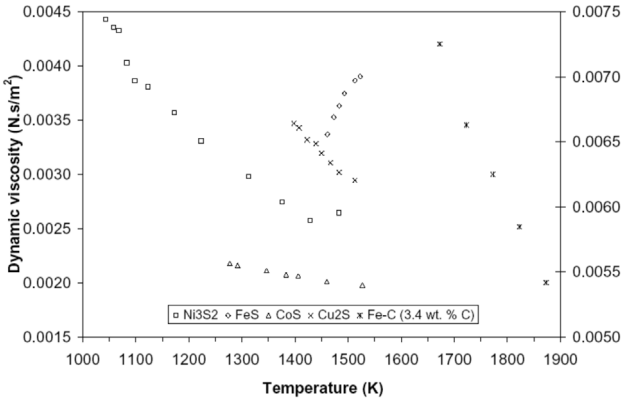

Figure 1—Dynamic viscosity of sulphide melts[1] (left axis) as well as pig iron (Fe-C) with 3.4 wt.% C[4] (right axis)

3.4 wt. % C) as a function of temperature is also shown, read off on the right axis[4]. The trends in Figure 1 were generated from the kinematic viscosity readings from Nikiforov *et al.*[1], which were converted to dynamic viscosity by using linear regression equations of density values from Kucharski *et al.*[5] in Equation [1].

$$v = \frac{\mu}{\rho} \qquad [1]$$

where v is the kinematic viscosity, μ the dynamic viscosity and ρ the density. Based on the minimal changes of density with temperature, it was assumed that the density measurements maintained a linear dependence on temperature even outside the temperature range used in the density investigation. A density value for Co_4S_3 from Dobrovinskii *et al.*[3] was used to determine the dynamic viscosity of the CoS compound. It was assumed that the density of the CoS would remain constant from 1 273 to 1 523 K because of the minimal dependence of matte density on temperature.

Trends for Ni_3S_2, CoS, and Cu_2S decreased almost linearly with an increase in temperature, while that of FeS increased unexpectedly. It is clear from Figure 1 that the dynamic viscosity of the pure sulphides is in the same order as that of pig iron, albeit somewhat lower. According to Nikiforov *et al.*[1], the increase in the viscosity of FeS with temperature may be the result of the formation of structural complexes and the enlargement of structural units in the matte. While it may seem strange to talk of structural units when referring to metallic liquids, liquid sulphide solutions are known to exhibit a high degree of short-range ordering[6].

For this reason successful thermodynamic models of liquid sulphides[7,6,8] have been developed using the modified quasi-chemical model of Pelton and Blander[9], which was originally used to thermodynamically model molten oxide (slag) systems[10,11], which are known as ordered liquids.

Interestingly, quasi-chemical models are now also used to model the viscosity of slags[12]. This seems to lend weight to Nikiforov's statement about structural units in the matte, as if these quasi-chemical models are used for both slag and matte thermodynamic modelling, as well as slag viscosity modelling, it seems that structural units could play a role in the viscosity of liquid sulphides.

Figure 2 contains viscosity isotherms for the pseudo-binary systems of Cu_2S-Ni_3S_2, FeS-Cu_2S, and FeS-Ni_3S_2. For the Cu_2S-Ni_3S_2 pseudo binary (Figure 2(a)) both viscosity isotherms show a minimum at roughly 90 wt. % Ni_3S_2, which is the eutectic composition for the Cu_2S-Ni_3S_2 pseudo binary[13,14]. Glazov and Vertman[15] have shown that viscosity minima often correspond to eutectic alloys where the bond strength between unlike particles, Cu_2S and Ni_3S_2 in this case, are weaker than those between like particles. When one considers the most extensive work done on the Cu-Ni-S system, done by Larrain and Lee[16] and Lee *et al.*[17], it is clear that there is liquid-liquid immiscibility in this system. This usually derives from the marked positive deviation from Raoult's law and there is thus a tendency towards repulsion of the different components, which results in extreme cases in liquid immiscibility as seen in the Cu-Ni-S system.

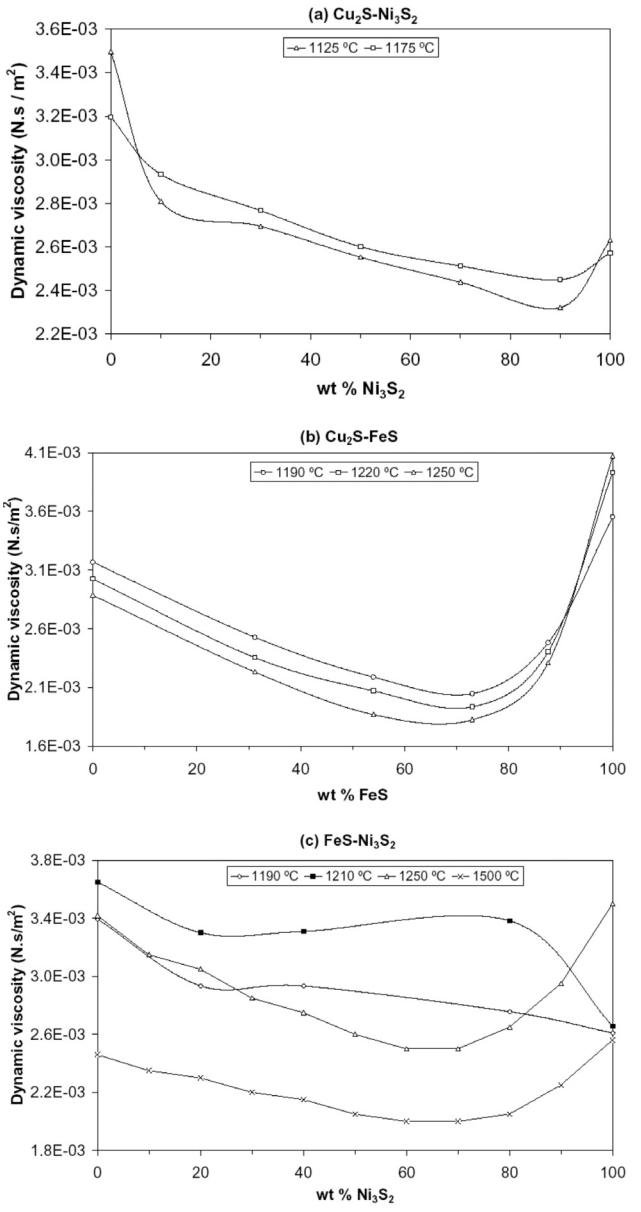

Figure 2—Viscosity-composition relationship of the systems: (a) Cu_2S-Ni_3S_2[1], (b) FeS Cu_2S[1], (c) FeS-Ni_3S_2[1,3]

The viscosity of the FeS-Cu_2S system (Figure 2(b)) decreased monotonically with temperature. Each of the viscosity isotherms for the FeS-Cu_2S system also haD a relatively broad minimum in the range 54–73 wt. % FeS. The FeS-Cu_2S system is also eutectic, with the eutectic composition at roughly 58 wt. % FeS[18,14]. The minima shown in Figure 2(b) is, however, not nearly as sharp as that seen in the Cu_2S-Ni_3S_2 system and it is therefore difficult to conclude whether the viscosity minima observed in Figure 2(b) is due to the eutectic or not.

The viscosity isotherms for the FeS-Ni_3S_2 system shown in Figure 2(c). This system shows peculiar viscosity behaviour with regard to temperature. Nikiforov *et al.*[1] state that for this system the viscosity smoothly decreases with an increase in temperature up to 1100–1150°C, above which there is an anomalous increase in viscosity. Unfortunately Nikiforov *et al.* do not show or reference any viscosity data for this system below 1190°C, so whether the viscosity actually decreases up to this point is not clear. From Figure 2(c) it is clear that the viscosity at 1190°C is lower than that at 1210°C. These were the two temperatures evaluated by Nikiforov *et al.*[1]. The 1250 and 1500°C isotherms then seem to show normal viscosity behaviour with regard to temperature, with the viscosity decreasing as the temperature increases. These two isotherms were compiled by Dobrovinskii *et al.*[3].

The reader may also notice a discrepancy between the viscosity of pure FeS at 1250°C when read off of Figure 2(c) and compared to the viscosity of pure FeS shown at the same temperature in Figure 1 (3.42×10^{-3} vs. 3.9×10^{-3} respectively). As mentioned the isotherms for the viscosity of the binary Ni_3S_2-FeS at 1250 and 1500 °C were obtained from Dobravinskii *et al.*[3], while the pure species data shown in Figure 1 are from the work done by Nikiforov *et al.*[1]. While there are no data available from Nikiforov *et al.*[1] for the viscosity of pure FeS at 1500°C, the value read off from Figure 2(c) at this temperature (2.46×10^{-3}) seems to buck the trend shown in Figure 1 for FeS, where the viscosity is found to increase with increasing temperature.

Viscosity trends for the FeS-Co_4S_3 and Ni_3S_2-Co_4S_3 systems are illustrated in Figure 3[3]. For both of these systems the viscosity decreases with an increase in temperature. Interestingly the FeS-Co_4S_3 system has a viscosity minimum close to 20% FeS, with the eutectic composition of this system being 25% FeS. The Ni_3S_2-Co_4S_3 system has a viscosity minimum around 30% Ni_3S_2.

If one compares all of the viscosity data for the sulphide mixtures to that shown for the Fe-C system in Figure 1 it is apparent that all of the sulphide melts reviewed in this paper have a lower viscosity than Fe-C. The viscosities of Fe-C and the sulphide melts are, however, of the same order.

Density

Knowledge of matte density is important for improving the accuracy of material balances in a smelter. Density data are useful for detecting solid spinel accumulation in smelting furnaces, which tends to accumulate at the slag-matte interface and is often tapped off with the matte. Thus, with reliable matte density data this could be detected by measuring the density of the molten matte when tapped from the furnace. Density data also find use in mass and heat transfer calculations. The settling rate of matte droplets through slag can be calculated, and temperature or concentration gradients cause density variations that result in natural convection within a melt. As with viscosity data, the knowledge of high-temperature density data is limited due to the experimental difficulties involved.

Experimental methods

Among the several methods used for measuring the density of molten mattes, four were investigated and their results compared. These methods are the bottom-weighing Archimedean technique[19], maximum bubble-pressure technique[20–22], U-tube method[23,24], and the sessile drop technique[25]. Hyrn *et al.*[26] evaluated many of the different methods. They found that the U-tube method is least accurate because the atmosphere above the matte sample cannot be purged. This gas that accumulates in this atmosphere may react with the melt and cause inaccuracies in the density measurements. The sessile drop technique is the simplest method to perform and allows measurement of density and surface tension at the same time, but may be slightly inaccurate due to the occurrence of small errors when analysing the image of the matte droplet. Accurate data can be obtained when using the maximum bubble-pressure technique, which also allows simultaneous measurement of density and surface tension. This method may, however, be very difficult to perform, because the sulphur pressure over the matte sample must be controlled. The bottom-weighing Archimedean technique is also reliable, because the sample-weight is continuously monitored. This means that compositional changes caused by sulphur can be detected.

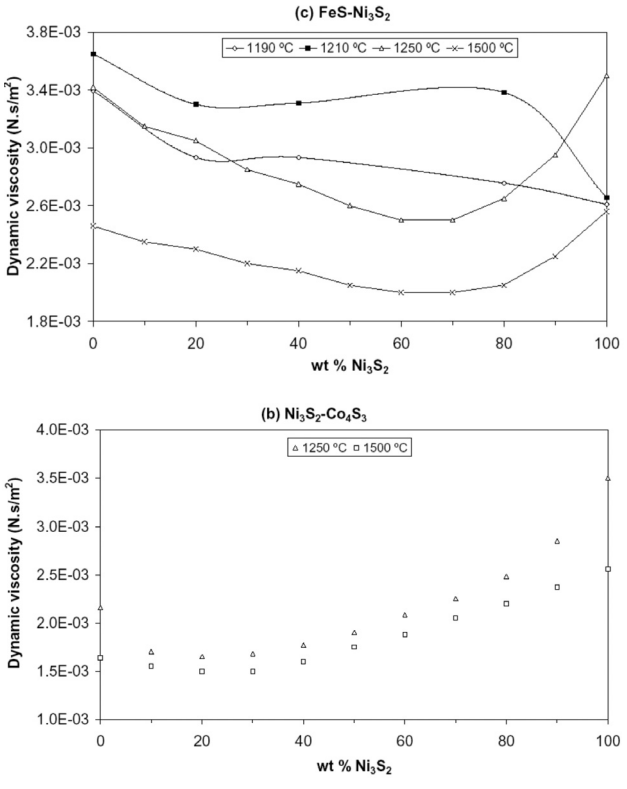

Figure 3—Viscosity-composition relationship of the systems: (a) FeS-Co_4S_3, (b) Ni_3S_2-Co_4S_3[3]

Density-temperature-composition relationships

Hyrn *et al.*[26] determined from their experimental results and by means of minimizing the sum of squares, an equation that quantifies the density of the Cu-Ni-Fe-S ternary system as a function of matte composition and temperature:

$$\tilde{n}_{matte} = 6.358 - 0.0763[S] + 9.940 \times 10^{-3}[Cu + Ni] - 4.645 \times 10^{-4}(T - 1000) \quad [2]$$

where the temperature is in °C and the relevant compositions in wt. %. Equation [2] was found to have a maximum error of 4.3% and is valid within the following ranges:

- 6.45 < [Cu] < 26.48
- 6.49 < [ni] < 30.18
- 23.6 < [S] ,30.1
- 0.43 < [O] , 3.57
- 13.3 < [Cu + Ni] < 57.0
- 0.88 < [Cu]/[Ni] < 1.02
- 14.1 < [Fe]/[O] < 36.6
- 1100 < T < 1300

Note that the use of Equation [2] for calculating densities of pseudo-binary systems may result in large errors of up to 15%. Hyrn *et al.*[26] quantified the densities of the following single-compound systems using linear regression:

$$\rho_{Ni_3S_2} = 6.144 - 6.6 \times 10^{-4} \cdot T \quad [3]$$

$$\rho_{Cu_2S} = 6.075 - 5.4 \times 10^{-4} \cdot T \quad [4]$$

$$\rho_{FeS} = 5.435 - 1.1 \times 10^{-4} \cdot T \quad [5]$$

where the density has units of g/cm³ and the temperature is expressed in K. Equations [3] through [5] are valid over a temperature range from 1273 to 1573 K. The small effect that temperature had on density in these equations indicates that density is not especially sensitive to changes in the temperature of molten matte within the specified temperature range. The linear models represented by Equations [3] through [5] compare relatively well with density data given by Tokumoto *et al.*[25] and Kaiura and Toguri[19], in which the sessile drop technique and a volume displacement technique were respectively used. Density data of the pseudo-binary systems, FeS-Ni_3S_2, Cu_2S-Ni_3S_2 and Cu_2S-FeS, from various sources are illustrated in Figure 9.

The system temperature was held constant at 1473 K for all the literature sources listed in Figure 4, excepting for the data from Dobrovinskii *et al.*[3] which were determined at temperatures between 1523 and 1723 K. These results were included because they agree with the other data and do not vary much with changes in temperature.

It is clear from Figure 4 that the results from Byerley and Takebe[23] are scattered. This behaviour is an attribute of the unreliable U-tube method used by Byerley and Takebe[23]. Their results do, however, maintain the general trend, but lack the accuracy of the results from the other investigators. The experimental method employed by Dobrovinskii *et al.*[3] and Kucharski *et al.*[5] is the maximum bubble-pressure technique. Ip and Toguri[27] made use of the sessile drop method. It appears that the spread of data in Figure 4 confirms that the maximum bubble-pressure technique and the sessile drop method are both reliable if performed correctly. The sessile drop technique is, however, not normally known for its accuracy in determining density data.

In Figure 4(a), the regressed density curve for the FeS-Ni_3S_2 system shows a significant decrease at high FeS concentrations.

The density data from Dobrovinskii *et al.*[3], Kucharski *et al.*[5] and Ip and Toguri[27] lie in a narrow band. The third order polynomial that passes through the data of Kucharski *et al.*[5] has an R^2 of 0.99 and overlays almost perfectly the data from Ip and Toguri[27]:

$$\rho_{FeS-Ni_3S_2} = -2.0417 \cdot X_{FeS}^3 + 1.4435 \cdot X_{FeS}^2 - 0.7618 \cdot X_{FeS} + 5.2014 \quad [6]$$

where the density is given in g/cm³ and the error is about 5%. The density of the Cu_2S-Ni_3S_2 system is essentially independent of composition. Data from all the literature sources listed in Figure 4(b) were regressed to give the following linear relationship with a maximum error of 10%:

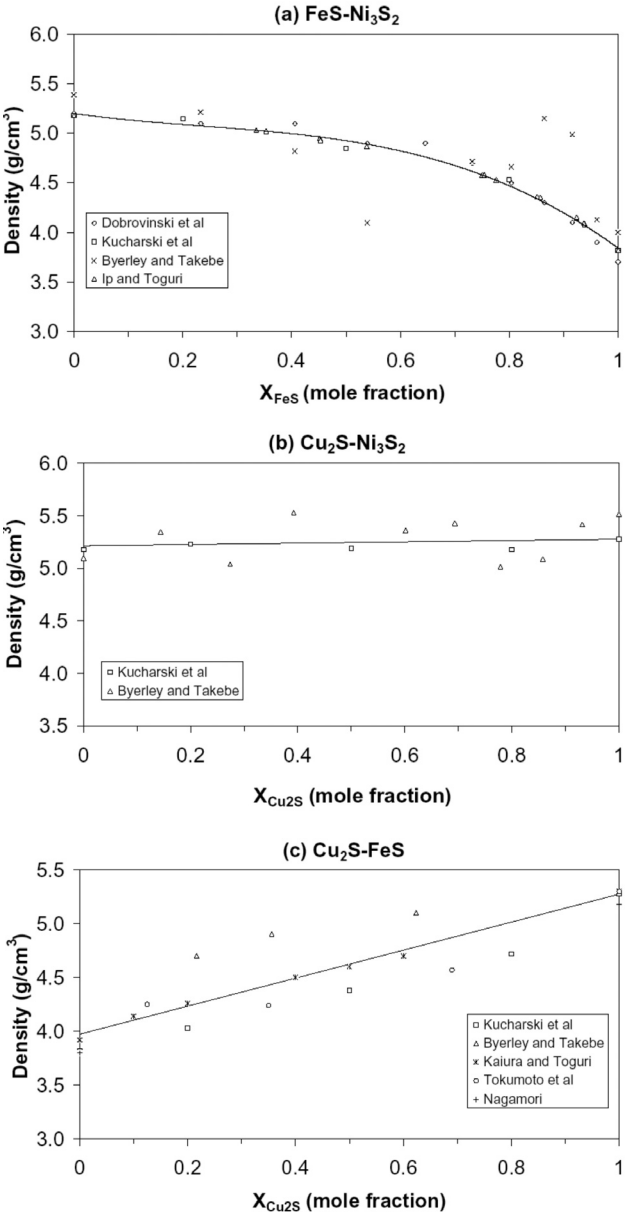

Figure 4—Density-composition plots at 1473 K for the systems: (a) FeS-Ni_3S_2, (b) Cu_2S-Ni_3S_2, (c) Cu_2S-FeS

$$\rho_{Cu_2S-Ni_3S_2} = 5.2152 + 0.0624 \cdot X_{Cu_2S} \quad [7]$$

When the results from the literature listed in Figure 4(c) were combined, then the following linear relationship emerged for the Cu_2S-FeS system:

$$\rho_{Cu_2S-FeS} = 3.9732 + 1.3012 \cdot X_{Cu_2S} \quad [8]$$

A 10% error may result in using Equation [8].

Byerley and Takebe[23] applied a least squares analysis to their experimental data to generate linear temperature-density equations. These equations revealed that the average drop in density for a 100°C temperature increase in the binary matte systems is about 0.2 g/cm³. If density data are available at a single temperature, then it would be reasonable to assume a density decrease of 0.2 g/cm³ if the temperature is raised by 100°C, or that the density would increase with 0.2 g/cm³ if the temperature is reduced by 100°C.

A ternary density diagram for the Ni_3S_2-Cu_2S-FeS system at 1473 K was reconstructed from Kucharski *et al.*[5] as shown in Figure 5. The addition of Cu_2S to the system has a weak effect on the matte density, especially when the matte is rich in Ni_3S_2. From Figure 5 it is apparent that the effect of FeS on the density of the pseudo-ternary becomes more significant at higher FeS concentrations. This is similar to the behaviour observed in the Ni_3S_2-FeS pseudo-binary system[5] (see Figure 4(a)).

Surface tension

Accurate measurement of surface tension is critical as its compositional sensitivity greatly affects slag/matte separation and the corrosive interaction of matte or slag with refractories. Reliable surface tension data would therefore assist in minimizing matte losses to slag and would be useful for designing refractory linings.

Experimental method

Only two methods were identified that have been used to measure the surface tension of mattes, namely the maximum bubble-pressure technique[28] and the sessile drop technique[28,29]. Both of these methods can be used to measure both density and surface tension simultaneously, as mentioned earlier. The relevant advantages and disadvantages of these two methods are also discussed earlier.

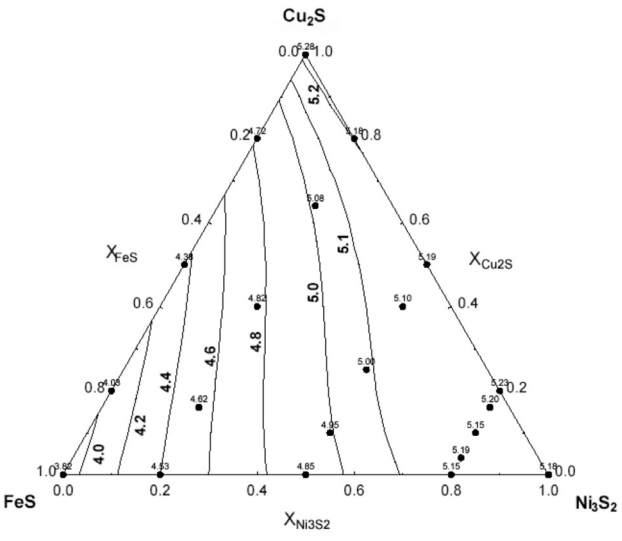

Figure 5—Ternary density diagram for the Ni_3S_2-Cu_2S-FeS system at 1473 K. Experimental values are represented by the closed circles and the solid lines are iso-density lines (g/cm³)[5]

Surface tension-composition-temperature relationships

The temperature dependence of the surface tensions for Ni_3S_2, Cu_2S, and FeS was measured by Kucharski *et al.*[5], see Figure 6 (left axis). Also shown in Figure 6 is the surface tension of pure liquid iron as a function of temperature (right axis). As was done with viscosity earlier, it is convenient to compare the surface tension of the sulphides to that of pig iron (Fe-C). The addition of carbon to liquid iron has been shown to have no effect on the surface tension of pure liquid iron[30,31], as such the surface tension of pure liquid iron[32] can be used to represent pig iron. It is clear from Figure 6 that the surface tension of pig iron is higher than that of the sulphides shown.

The temperature span for pure Cu_2S and FeS is less than the 300 K range for Ni_3S_2 because of their higher melting points. Cu_2S and FeS show negligible temperature dependency and maintain approximate values of 0.39 and 0.328 N/m respectively. The surface tension of Ni_3S_2 decreases linearly with increasing temperature[5]:

$$\gamma_{Ni_3S_2} = 0.826 - 0.0002 \cdot T \quad [9]$$

where γ is the surface tension in N/m (as is the case for all the expressions for surface tension in this section) and T the temperature in K. The surface tension measurements of FeS in Figure 6 compare well with those from Tokumoto *et al.*[25] and the results for Cu_2S deviate by approximately 10%. This difference may be the result of compositional variations and the difference between the experimental methods.

Hengzhong[33] developed a useful equation, from first principles of thermodynamics:

$$\frac{1}{\gamma^n} = \sum \left(\frac{a_i}{\gamma_i^\circ} \right)^n \quad (n > 0) \quad [10]$$

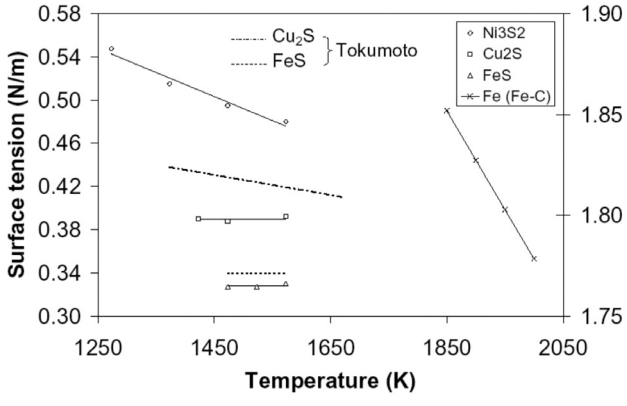

Figure 6—Effect of temperature on surface tension of pure matte compounds[5] (left axis) and pure Fe liquid[32] (right axis). Dashed lines represent data from Tokumoto *et al.*[25]

where:

γ = solution surface tension (N/m)

a_i = activity of component i

γ_i° = surface tension of pure component i (N/m)

n = shape factor

Hengzhong[33] assigns positive integer values to the shape factor n until the calculated surface tension values for a specific system correspond fairly well with experimentally determined data of the same system.

Krivsky and Schuhmann[34] pointed out that it is reasonable to see ordinary copper mattes as ideal solutions of Cu_2S and FeS when accurate activity data are not available. Equation [10] can therefore be written as follows:

$$\frac{1}{\gamma^n} = \sum \left(\frac{x_i}{\gamma_i^\circ} \right)^n \quad (n > 0) \qquad [11]$$

where x_i is the molar fraction of component i. The only input requirement of Equation [11] for pseudo-binary matte systems is an accurate value for the surface tension of each pure component, and an estimate of the n value, which is normally set to unity for Cu-Ni-Fe-S mattes. Equation [11] may be useful when no knowledge other than the surface tension of each pure component is available. The trend predicted by this equation may not always adopt the perfect shape and is sometimes more linear than what it should be. Hengzhong[33] compares the result of Equation [11] with only one set of experimental data. This approach may not be the best practice, since the experimental error involved when comparing the results of surface tension between different investigators is approximately 10%. Large errors occur as a result of the sensitivity of surface tension measurements to temperature and compositional variation.

Equation [10] would be very useful for determining values for surface tension that are accurate if reliable activity data are available for a specific matte system. Since it is more difficult to experimentally determine activity data, Equation [10] may be used to determine activity data for a system from reliable surface tension data. Reliable expressions for calculating the surface tensions of Ni-Fe-S and Ni-Cu-S matte systems were developed from the experimental data of Ip and Toguri[27]. Their equations are useful because the only input criteria are elemental compositions. The equation for the Ni-Fe-S system had a correlation coefficient of 0.999 and is written as follows:

$$\begin{aligned} \gamma_{Ni-Fe-S} &= 0.649 \cdot X_{Ni} + 0.436 \cdot X_{Fe} + 0.162 \cdot X_S \\ &= 0.162 + 0.487 \cdot X_{Ni} + 0.274 \cdot X_{Fe} \\ &= 0.649 - 0.213 \cdot X_{Fe} - 0.487 \cdot X_S \\ &= 0.436 + 0.223 \cdot X_{Ni} + 0.264 \cdot X_S \end{aligned} \qquad [12]$$

A regression analysis for the data of the Ni-Cu-S system has a correlation coefficient of 0.89:

$$\begin{aligned} \gamma_{Ni-Cu-S} &= 0.429 \cdot X_{Ni} + 0.312 \cdot X_{Cu} + 0.524 \cdot X_S \\ &= 0.429 + 0.117 \cdot X_{Cu} + 0.095 \cdot X_S \\ &= 0.524 - 0.095 \cdot X_{Ni} - 0.212 \cdot X_{Cu} \end{aligned} \qquad [13]$$

Ip and Toguri[27] commented that if the coefficients in Equation [12] are compared, it can be numerically concluded that sulphur has the greatest influence on the surface tension of the nickel-iron matte, with the coefficient of sulphur being roughly 18% higher than nickel. They also concluded, using Equation [12], that addition of sulphur (with negative coefficient) to the matte will decrease the surface tension of the system. Similarly, Equation [13] indicates that Cu addition tends to decrease the surface tension of the melt.

Equations that relate surface tension with pseudo-binary systems based on Equations [12] and [13] respectively are:

$$\gamma_{Ni_3S_2-FeS} = \frac{2.271 - 1.673 \cdot X_{FeS}}{5 - 3 \cdot X_{FeS}} \qquad [14]$$

$$\gamma_{Ni_3S_2-Cu_2S} = \frac{1.188 \cdot X_{Ni_3S_2} + 1.149}{2 \cdot X_{Ni_3S_2} + 3} \qquad [15]$$

Equations [12] and [14]were derived from compositional data near that of the Ni_3S_2-FeS pseudo-binary system. Similarly, Equations [13] and [15] were developed from data with compositions near that of the Ni_3S_2-Cu_2S pseudo-binary. Equations [14] and [15] are shown as curves in Figure 7 and Figure 8 and do not represent the spread of data particularly well. This may be because of slight elemental deficiencies in the pseudo-binary samples from which these equations were determined[27].

The spread of data for the Cu_2S-FeS pseudo-binary system is illustrated in Figure 7. The data from Elliott and Mounier[35] and from Kucharski *et al.*[5] were obtained using the maximum bubble-pressure technique. Their data displays a similar trend, but differ with a maximum error of 5%, which may be from experimental and compositional differences. Results from Vanyukov *et al.*[36] have a linear spread and those from Tokumoto *et al.*[25] (sessile drop technique) appear to be more irregular. The Henzhong

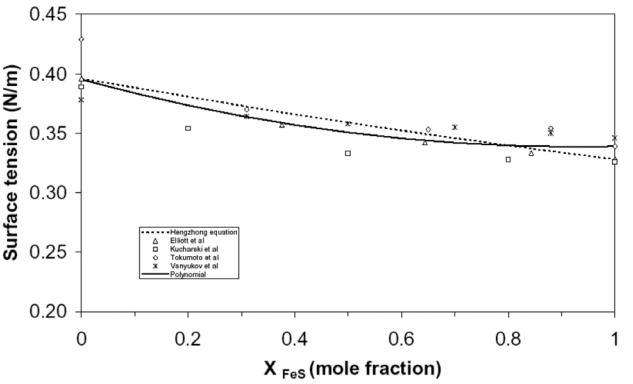

Figure 7—Comparison of surface tension data at 1473 K for Cu_2S-FeS

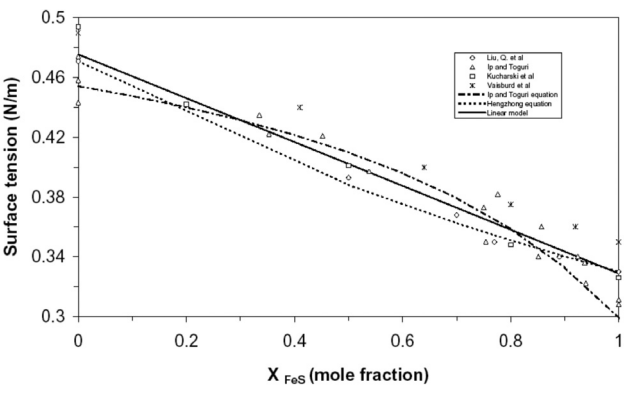

Figure 8—Comparison of surface tension data at 1473 K for Ni_3S_2-FeS

Equation [33] appears to be linear and may not have the most appropriate fit. A second order polynomial represents the system well (solid line in Figure 7) and has an R^2 of 0.73:

$$\gamma_{Cu_2S-FeS} = 0.0657 \cdot X_{FeS}^2 - 0.122 \cdot X_{FeS} + 0.3952 \quad [16]$$

The average error that can be expected when using this equation is about 8%. Figure 8 illustrates the Ni_3S_2-FeS pseudo-binary system. Data from all literature appears to be linear, except for the curved spread of data from Ip and Toguri[27] which are well matched with Equation [14]. All data nevertheless agree very well and can be regressed with a linear model (R^2=0.93):

$$\gamma_{Ni_3S_2-FeS} = 0.4755 - 0.1467 \cdot X_{FeS} \quad [17]$$

An average error of up to 9% may occur when using this equation. The data in Figure 9 (Cu_2S-Ni_3S_2 system) are also not represented well with the Hengzhong equation (Equation [11] or Equation [15] from Ip and Toguri[27]).

The following second order polynomial gives the best fit for the data in Figure 9; it has an R^2 of 0.77 and may have an average error of 10%:

$$\gamma_{Ni_3S_2-Cu_2S} = 0.0983 \cdot X_{Ni_3S_2}^2 - 0.0253 \cdot X_{Ni_3S_2} + 0.4027 \quad [18]$$

Hengzhong[33] also proved that Equation [11] is very useful for accurately predicting the surface tension of Pb-Cu-S and Pb-Fe-S systems. The information required to calculate surface tensions for these systems with this equation is $\gamma_{PbS} \approx 0.2$ N/m and the parameter $n = 1$. An important parameter to consider when selecting and designing refractory linings for furnaces is the contact angle between a specific refractory substrate and molten slag. The contact angles between Ni-Cu-S matte (at 1473 K) and the different refractory materials investigated in Ip and Toguri[27] display no particular relationship with a change in Ni_3S_2 concentration and randomly varies between angles of 95 to 150 degrees. The refractory materials can be identified in Figure 10. A definite linear relationship occurs between the contact angle and the Ni_3S_2 concentration of a matte droplet for each refractory material.

The linear relationships between the contact angle $\grave{e}$ (in degrees), and Ni_3S_2 concentration of the Ni-Fe-S system as from Figure 10 are listed as follows.

$$\text{Silica}: \quad \theta_{silica} = 13.6 \cdot X_{Ni_3S_2} + 128.93 \quad [19]$$

$$\text{Alumina}: \quad \theta_{alumina} = 56.033 \cdot X_{Ni_3S_2} + 85.673 \quad [20]$$

$$\text{Magnesia}: \quad \theta_{magnesia} = 40.048 \cdot X_{Ni_3S_2} + 76.629 \quad [21]$$

$$\text{Sapphire}: \quad \theta_{sapphire} = 101.41 \cdot X_{Ni_3S_2} + 68.217 \quad [22]$$

$$\text{C1215}: \quad \theta_{C1215} = 56.915 \cdot X_{Ni_3S_2} + 52.804 \quad [23]$$

where C1215 is a 94.2 wt. % Cr_2O_3–3.8 wt. % TiO_2 refractory. From Figure 10 it is apparent that regardless of the substrate used, the contact angle between the drop and the substrate increases with an increase in nickel sulphide content in the matte. As such the wetting of the solids by matte is favoured by high iron sulphide contents. The wetting behaviour of the solid oxides by nickel matte can be ranked in order of increasing wettability as follows[27]:

$SiO_2 < Al_2O_3 \leq$ sapphire $\leq MgO < C1215$

Ip and Toguri[27] proposed an equation that predicts the surface tension behaviour of the Cu_2S-Ni_3S_2-FeS pseudo-ternary from the available surface tension data on the Ni_3S_2-FeS and Ni_3S_2-Cu_2S pseudo-binary systems (see Equations. [14] and [15]):

$$\gamma_{Ni_3S_2-Cu_2S-FeS} = t \cdot \gamma_{Ni_3S_2-FeS} + (1-t) \cdot \gamma_{Cu_2S-FeS} \quad [24]$$

$$\text{where } t = \frac{X_{Cu_2S}}{X_{Ni_3S_2} + X_{Cu_2S}} \quad [25]$$

Ip and Toguri[27] are, however, unclear on the specifics of how this equation should be used. Their result (see Figure 11) slightly resembles the pseudo-ternary system developed directly from the experimental ternary data of Kucharski *et al.*[5] shown in Figure 12.

When one assesses the iso-surface tension lines shown in Figure 12, it is apparent that they radiate out from the Ni_3S_2 corner of the diagram. This indicates that the surface tension in this system is most sensitive to the concentration of Ni_3S_2. Using a similar argument it is clear that the addition of Cu_2S to the system does not affect the surface tension significantly, as the iso-surface tension lines tend to point towards the Cu_2S corner[5].

Yan *et al.*[37] compared models for the surface tension of the Ni_3S_2-FeS-Cu_2S system by using the data from Kucharskii *et al.*[5]. Yan *et al.* used two geometric models (the Kohler and Toop models[38]) as well as a general solution model (Chou model[39]). They then also drew ternary surface

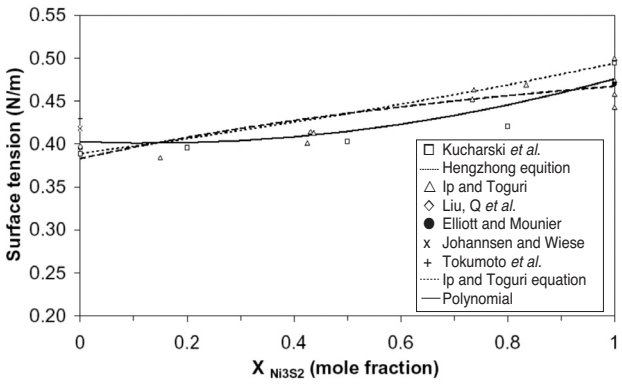

Figure 9—Comparison of surface tension data at 1473 K for Cu_2S-Ni_3S_2

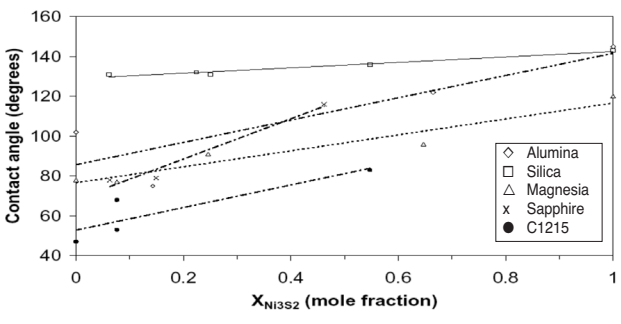

Figure 10—Contact angle of Ni_3S_2-FeS matte on various substrates at 1473 K

diagrams for the surface tension for each model. The ternary diagrams representing the different models used by Yan *et al.* all have a slightly different character to that shown in Figure 12 in that the iso-surface tension lines do not radiate out from the Ni_3S_2 corner of the diagram. The models that they fit all performed relatively well but are perhaps slightly complicated. For this reason it is preferred to fit a cubic polynomial to the data of Kucharskii *et al.*, which is shown in Equation [26].

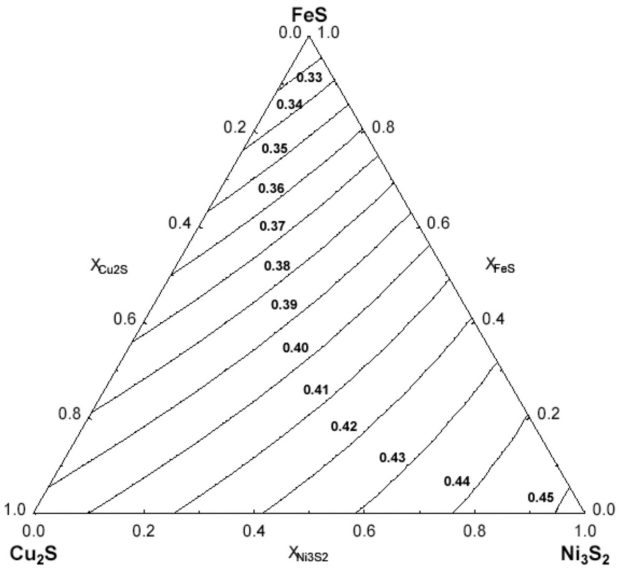

Figure 11—Ternary surface tension diagram for the Ni_3S_2-Cu_2S-FeS system at 1473 K according to the theoretical approach of Ip and Toguri[27] (N/m)

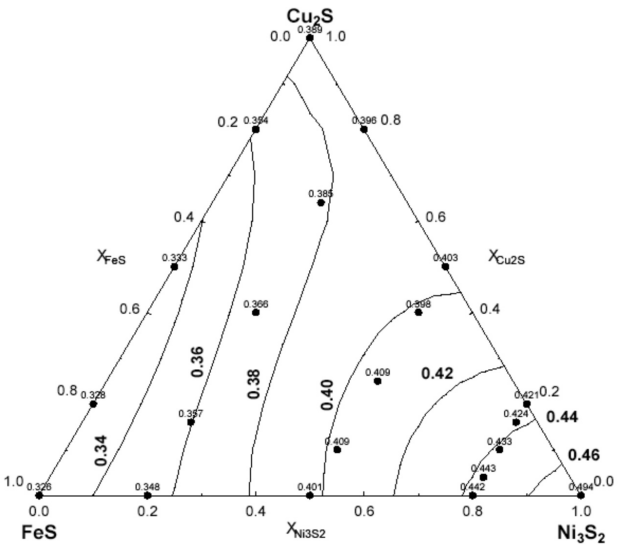

Figure 12—Ternary surface tension diagram for the Ni_3S_2-Cu_2S-FeS system at 1473 K according to the experimental data of Kucharski *et al.*[5] Experimental points are represented by the closed circles and the solid lines are iso-tension lines (N/m)[5]

$$\gamma_{Ni_3S_2-Cu_2S-FeS} = 0.327 \cdot X_{FeS} + 0.4759 \cdot X_{Ni_3S_2} + 0.3945 \cdot X_{Cu_2S} - 0.0197 \cdot X_{FeS} \cdot X_{Ni_3S_2} - 0.1157 \cdot X_{FeS} \cdot X_{Cu_2S} - 0.1627 \cdot X_{Ni_3S_2} \cdot X_{Cu_2S} + 0.5672 \cdot X_{FeS} \cdot X_{FeS} \cdot X_{Ni_3S_2} \cdot X_{Cu_2S} \quad [26]$$

Equation [26] performs very well when compared to the experimental data of Kucharskii *et al.*, with an R^2 value of 0.97 and an average mean squared error of 1.55%, which is below the experimental error reported by Kucharskii *et al.* of 2.5%. Equation [26] out performs the models evaluated by Yan *et al.*[37] and is also considered to be simpler to use.

For a FeS-Cu_2S-PbS pseudo-ternary system with low concentrations of PbS (0.1 to 0.2 mole fraction), the mixture formed by FeS and Cu_2S may be treated as an ideal solution. The system may also be regarded as a dilute solution of PbS. The activity coefficients of FeS and Cu_2S are assumed to be 1 and that of PbS is r_{PbS}. With these assumptions and with n = 1, the Hengzhong equation (Equation [10]) gives results, which agree very well with experimental data. It is important to realize that simplification of the Hengzhong equation to a form such as Equation [11] may give accurate results only if it is reasonable to assume that a system is ideal.

Interfacial tension

As for surface tension, interfacial tension may greatly affect phenomena such as entrainment of matte into slag and the flotation of minerals with gas. For example, if the interfacial tension between a slag and metal phase is low then molten slag could easily become entrapped in the metal. Similarly, if the interfacial tension between the phases is high, bubbles could become entrapped in the metal phase resulting in defects on solidification[28].

Experimental method

The measurement of interfacial tension is also done using the sessile drop technique. In this case the drop of molten matte is submerged in molten slag. By observing the profile of the matte droplet (usually using X-ray) the interfacial tension can be determined[27]. Problems associated with this method include the fact that it is extremely difficult to perform the experiments in a sample holder (crucible) which does not interact with the matte-slag system[27]. The duration of the experiment is thus limited to minimize the dissolution of the crucible. Ip and Toguri[27] also experienced problems with bubble formation due to reactions between the matte and slag.

Interfacial tension-composition relationships and contact angles

Equation [27] was proposed by Girifalco and Good[40]. It relates the interfacial tension with the surface tension of two phases.

$$\gamma_{12} = \gamma_1 + \gamma_2 - 2\phi\sqrt{\gamma_1 \cdot \gamma_2} \quad [27]$$

ϕ = Girifalco-Good interaction parameter
γ_{12} = interfacial tension (N/m)

γ_1 = surface tension of phase 1 (N/m)
γ_2 = surface tension of phase 2 (N/m)

where ϕ can be calculated from the molar volumes of the contacting liquids[27]. For the experimental work done by Ip and Toguri[27] this proved to be problematic as for the matte and slag used in their study it was difficult to define the molecular mass of the liquids as the melts tend to be non-stoichiometric. By definition, ϕ is a function of the adhesive and cohesive forces exerted on the molecules in the liquids. The exact relationship is shown below[27]:

$$\phi = -\frac{F_{ab}^{a}}{\left(\Delta F_{a}^{c} \cdot \Delta F_{b}^{c}\right)^{1/2}} \quad [28]$$

$$F_{ab}^{a} = \gamma_{12} - \gamma_1 - \gamma_2 = \text{force of adhesion between phases A and B, per unit area} \quad [29]$$

$$F_{n}^{c} = 2\gamma_n = \text{force of cohesion for phase N} \quad [30]$$

When the cohesive and adhesive forces between the molecules are similar, then ϕ approaches a value of 1. Ip and Toguri[27] found that ϕ is a linear function of matte composition and approaches a value of 1 as the composition of the matte approaches that of pure FeS (see Figure 13). They mention that this increase is to be expected, since iron is a main component of the fayalite slag and increasing the iron content in the matte would increase the similarity in the bonding forces between the two phases.

Experimental results for interfacial tension at 1473 K from Ip and Toguri[27] are shown in Figure 14. Samples were treated in magnesia and alumina crucibles and the average Fe/SiO_2 (wt/wt) ratio of the slag was around 1.58. The interfacial tension data from Zaitsev *et al.*[41] are also displayed in Figure 14. Deviation of the data points of Zaitsev *et al.*[41] from those of Ip and Toguri[27] may be due to the increased treatment temperature (1523 K) and the higher Fe/SiO_2 (wt/wt) ratio (1.86) in Zaitsev *et al.*[41]. A regression model for the data in Figure 14 (with interfacial tension in N/m and X in mole fraction), with a correlation coefficient of 0.976, written in terms of the elemental analysis, is given as:

$$\gamma_{Ni-Fe-S/slag} = 0.454 \cdot X_{Ni} + 0.123 \cdot X_{Fe} - 0.228 \cdot X_{S} \quad [31]$$

A modified version of Equation [31] based on stoichiometric Ni_3S_2 and FeS is given as:

$$\gamma_{Ni_3S_2-FeS/slag} = \frac{0.907 - 1.013 \cdot X_{FeS}}{5 - 3 \cdot X_{FeS}} \quad [32]$$

In both Equations [31] and [32] the interfacial tension is expressed in N/m and X in mole fraction. Interfacial tension tends to decrease with decreasing matte grade. The presence of magnesium oxide and aluminium oxide in the matte had no observable effect on surface and interfacial tension[27].

Elliott and Mounier[35] found that the interfacial tension between matte and slag systems increased almost linearly from 0.02 to 0.1 N/m when the copper grade was increased from 0 to 80 wt.%. Similarly, Mandira *et al.*[29] found that the interfacial tension between matte and slag increased almost linearly from 0.07 to 0.12 N/m when the FeO/SiO_2 (wt/wt) ratio was increased from 1.6 to 2.4 for a matte with a copper content of 46.4 wt.%. Mungall and Su[42] evaluated the interfacial tension between liquid Cu-Fe-Ni-S and Fe-S-O melts and basaltic melts at temperatures ranging from 1250–1325°C. They found that the effect of temperature was negligible relative to the precision of the experiments. In terms of the effect of the sulphide melt composition they found that the addition of Cu and Ni to the FeS melt lead to an increase in the interfacial tension, with a 6.5 wt.% addition of Ni or 16 wt.% addition of Cu leading to a 20% increase in the interfacial tension. They also found that the addition of up to 3.9 wt.% oxygen to the FeS melt had no effect on the interfacial tension.

The contact angle of nickel mattes on alumina and magnesia in the presence of slag at 1473 K is illustrated in Figure 15. It is clear from the large contact angle shown in this figure that alumina and magnesia are wetted by liquid slag[27].

Electrical conductivity

Particle selection techniques and smelting operations may be reliant on the electrical properties of the minerals being handled. In pyrometallurgy, when working with slag resistance furnaces, the amount of power required to melt minerals is strongly related to the resistivity of the molten materials. While traditionally only the conductivity of the slag

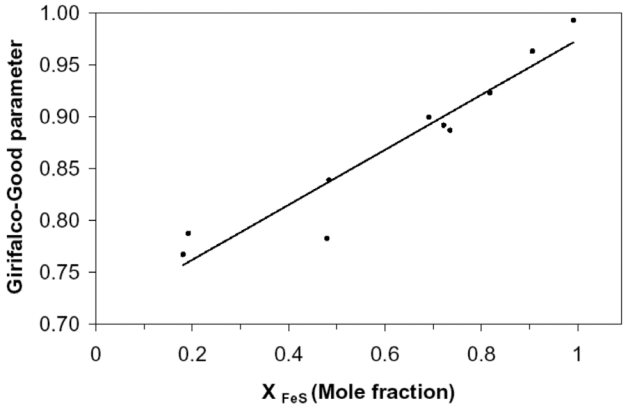

Figure 13—The Girifalco-Good parameter for the Ni-Fe-S/Fe-SiO_2 system at 1473 K

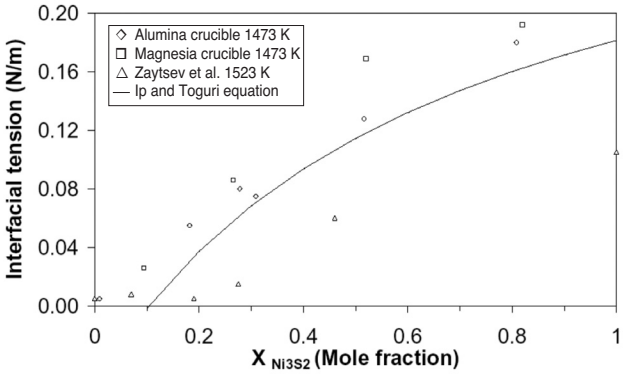

Figure 14—Interfacial tension between nickel-iron matte and fayalite slag as a function of matte composition at 1473 K. The solid line represents the calculated curve for the Ni_3S_2-FeS pseudo-binary[27]

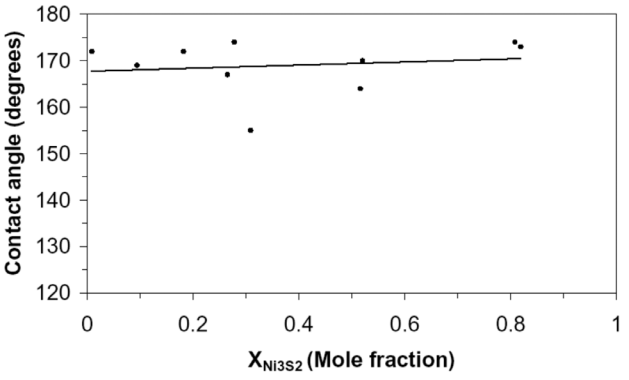

Figure 15—Contact angle between Ni-Fe-S matte and alumina and magnesia in the presence of slag at 1473 K[27]

phase in these furnaces has been of interest, the conductivity of the matte also has a large role to play in electrical furnace operation, as it has been shown that much of the current actually flows through the matte[43]. This, combined with dangers associated with extreme matte overheating, make it important that the electrical conductivity of the matte is known.

The electrical conductivity (or specific conductivity) of a material is directly related to the type of bonding and bond strength between the atoms in the crystal[44]. The electrical properties of metallic materials are very different from materials that are bonded covalently or ionically. Conductivities of metallic materials are generally high as a result of the mobility of the clouds of electrons surrounding the positively charged metal nuclei.

In covalently bonded structures such as silica, electrons are confined to move within certain electron bands, and directional bonds are formed between the electron bands of neighbouring atoms. This limits the ease of electron transfer throughout the crystal structure of the material and results in low electrical conductivity. Electrical conductivities of ionic solids vary according to the strength with which electrons are held in the outer electron shell of an ion. Transfer of electrons between ions causes a difference in the net charge of each of the atoms. This results in an attractive force which will hold the solids together. Because no solid has a completely ordered structure defects can occur through misplaced or missing atoms or electrons. The population and mobility of these defects will determine the electrical conductivity of the solid. When a material contains ions in which it is difficult to add or remove an electron the population of electron defects will be low and in this case the mechanism of transfer of electrical charge will be via the diffusion of the ions in the solid. While there are many ions they have extremely low mobilities in most structures and therefore the electrical conductivities of the solids are low[44].

In semiconducting materials that contain elements with similar energies of ion exchange, electron defects may be transferred between neighbouring ions quite easily. These solid materials are therefore good electrical conductors, but are not as good as metallic solids, hence the name semiconductor. From the above discussion it is clear that electrical properties of materials can be extremely sensitive to the presence of impurities and lattice defects. Also, the ore structure will have a larger effect on the resistivity of composite materials than the proportion of conductive minerals they contain[44].

It may seem out of place to consider the electrical properties of solids when this paper is focused on liquid mattes. However, the work done over a hundred years ago by Kirchhoff and de la Rive, where they measured the electrical resistance of several metals just above and below their melting points, indicated that the ability of metals to conduct electricity is relatively unaffected by the transition from the solid to the liquid state[45]. The mechanisms of conductance as described above are as valid for liquids as they are for solids, for example, liquid copper is a metallic conductor, while liquid NaCl is an ionic conductor.

Liquid metal sulphides are generally either metallic- or semi-conductors; however, exact classification between the two has received much attention over the years, as described by Enderby and Barnes[45] in what is probably the most extensive study on liquid semiconductors ever published. Going into the details of the exact classification between metallic- and semi-conducting materials is, however, beyond the scope of this paper and the reader is referred to the paper by Enderby and Barnes[45]. A general rule of thumb is related to the effect that temperature has on the conductivity of the liquid in question. Generally, a decrease in conductivity with an increase in temperature is indicative of a metallic conductor, while an increase in conductivity with temperature is indicative of a semiconducting material.

Experimental method

While the details may vary, most research done in the measurement of the electrical conductivity of mattes was performed in roughly the same manner. Almost all measurements were done using alternating current circuits with either 2 terminals[46–48] or 4 terminals[49–51]. Alternating current circuits were preferred as they eliminated the possible effect of electrode reactions that could occur when using direct current.

Of the papers reviewed, only Dancy and Derge[52] used a direct current circuit. They did, however, make double measurements for each set of conditions, with the polarity reversed. The conductivity was then calculated using the average of the two readings. They postulated that this technique would eliminate errors caused by thermal electromotive forces produced at the junctions of the electrodes and leads. Although these junctions were constructed identically, and were in the same temperature zone, they found that on practice considerable error was introduced if readings were taken with the current passing in one direction only.

All of the papers reviewed used the concept of the cell constant to calculate the conductivity of the samples. The cell constant for each cell was firstly determined using a fluid of known conductivity such as H_2SO_4[50,49,51], KCl[47] or mercury[52]. The cell constant was then calculated by measuring the resistance when passing current through these solutions at room temperature, with the assumption that the geometry of the cell did not change much at high temperatures due to the low expansion coefficient of the materials of construction of the cells. The cell constant (k [cm^{-1}]) was then calculated using the measured resistance (R [Ω]) and conductivity of the solution (σ [$\Omega^{-1}cm^{-1}$]) from the following equation:

$$k = \sigma \cdot R \quad [33]$$

Equation [33] was then used to calculate the conductivity of the matte using the determined cell constant and the resistance measured during the actual experiments.

Electrical conductance-temperature-composition relationships

The behaviour of Cu-S systems with increasing sulphur content at different temperatures is illustrated in Figure 16. Two regions are clearly identifiable in Figure 16. On the copper rich side—i.e. the region left of stoichiometric Cu_2S (20.15% sulphur)—the electrical conductance is constant and independant of sulphur content, while an exponential dependence can be seen to the right of stoichiometric Cu_2S. Enderby and Barnes[53] state that CuS is a metallic conductor (as is pure Cu), and Cu_2S is a semiconductor, which may explain the behaviour shown in Figure 16. Exponential dependence of electrical conductivity on sulphur content was regressed for sulphur rich Cu-S to the right of stoichiometric Cu_2S. These relationships based on all the data shown are given below:

$$\sigma_{Cu_2S} = 60.6 \quad \leq 20.15\% \text{ sulphur} \quad [34]$$

$$\sigma_{Cu_2S} = 3.7 \times 10^{12} \exp^{1.51[S]} \geq 20.15\% \text{ sulphur} \quad [35]$$

σ = electrical conductivity ($\Omega^{-1}cm^{-1}$)
[*S*] = sulphur composition in mass %

The region between the two vertical lines indicates the most probable spread of data for copper-rich Cu-S according to Dancy and Derge[52]. Their investigations also indicated a narrow error band for a Cu-S melt that is rich in sulphur. It is difficult to justify this conclusion against the data of Bourgon *et al.*[54] which tend to have higher and more erratic conductivity values in sulphur-rich Cu-S.

A strong dependence of electrical conductivity with temperature is noticeable for sulphur concentrations up to 20.15%, while it is difficult to identify a meaningful temperature relationship above 20.15% sulphur. It is noticeable that the electrical conductivity increased sharply from 60 to 370 ($\Omega^{-1}cm^{-1}$) for an increase in sulphur content of only 1.5%. It may therefore be concluded that Cu-S matte is particularly sensitive to sulphurous impurities, which cause the sulphur content to exceed the stoichiometric concentration of sulphur in pure Cu_2S.

The data in the sulphur-rich region of Figure 16 originated from Bourgon *et al.*[54] and Dancy and Derge[52]. Their results followed a similar trend but started to diverge with increasing sulphur content. The experimental apparatus used by Dancy and Derge[52] was a four-terminal cell with a dc potentiometric circuit, whereas Bourgon *et al.*[54] used a four-terminal cell with an ac potentiometric circuit. Pound *et al.*[49] made use of an ac potentiometric circuit to eliminate the occurrence of electrode reactions when dc current was supplied. This may be the reason for the difference observed. Data points situated in the Cu-rich region agree well and may have a deviation of about 20% at each temperature. Electrical conductivity in the sulphur-rich region may deviate by 50% or even more at a specific temperature. All the data points, including individual data points from Yang *et al.*[55] and Enderby and Barnes[53], situated at the sulphur compositionof stoichiometric Cu_2S agree well in relation to the temperatures at which the data were measured.

Results of the temperature dependence of electrical conductance for pure Cu_2S are illustrated in Figure 17. It may be assumed that these results are also valid for Cu-S with a sulphur content ranging from 19 to 20.15 weight %, i.e. sulphur deficient Cu_2S and stoichiometric Cu_2S.

All the trend lines have a positive temperature coefficient, meaning that electrical conductivity increases with temperature. The four trend lines that are not from Knacke and Strese[47] lie within reasonable proximity of each other and were all obtained using four-terminal potentiometric cells. The four trend lines from Knacke and Strese[47] were determined with a two-terminal cell and have lower conductivity values than the trends from the other literature sources. This was possibly the result of a significant lead resistance in the two-terminal circuit, although differences in operating conditions and experimental errors may also have been a probable cause of deviation.

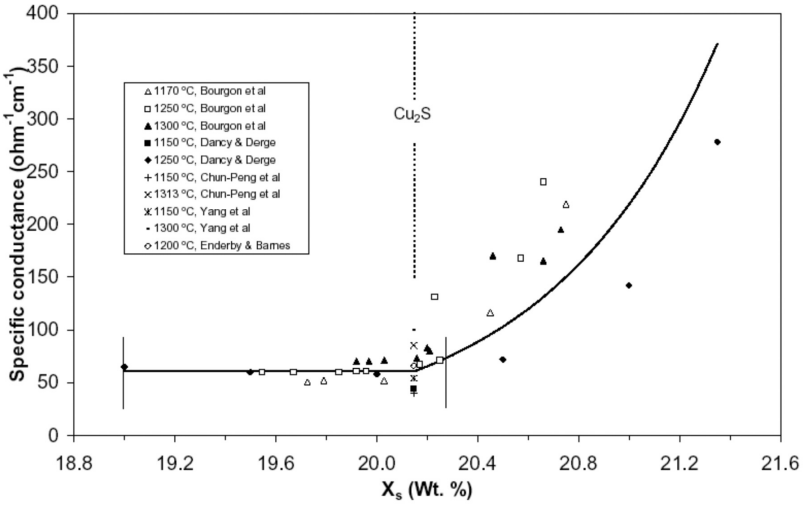

Figure 16—Electrical conductivity of the Cu-S system at various sulphur concentrations

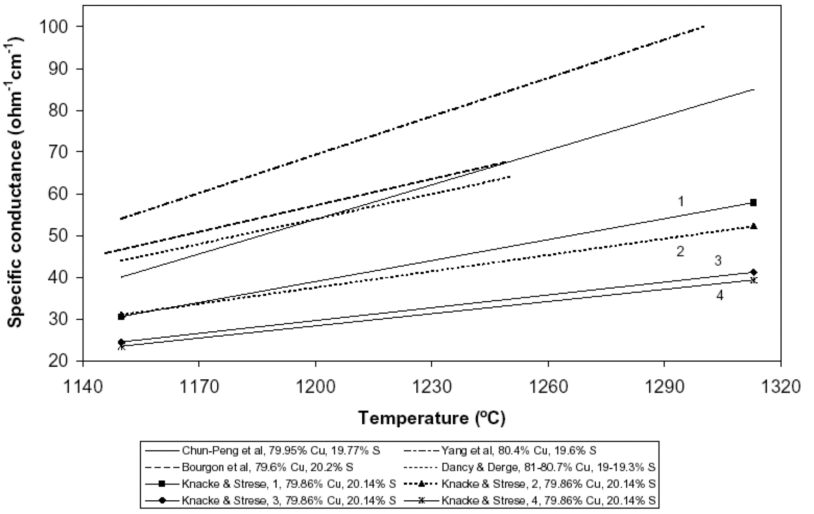

Figure 17—Temperature dependence of the electrical conductivity of Cu_2S

The four trends from Knacke and Strese[47] show that conductivity decreased as the duration of heat treatment on a molten sample increased. Curve 1 was measured immediately after melting finely milled Cu_2S and the measurements were recorded while the melt temperature was decreasing at a high cooling rate. The measurements of Curve 2 were recorded after a longer heating time. Curves 3 and 4 were measured after heating Cu_2S for one hour (even longer) in an argillaceous and a carbon crucible, respectively. The increased time of heating for Curves 3 and 4 caused a decrease in stoichiometric copper content from 79.86 to 79.6%. This may have been the result of a shift in the melt composition towards high temperature Cu1.8S, according to Knacke and Strese[47].

Conductivity measurements were recorded by Bourgon *et al.*[54] only after four hours of heat treatment when the conductivity of the matte remained constant. Stoichiometric Cu_2S proportions were continually maintained throughout their experiments by means of H_2S gas control. The length of time of experimentation did not affect the conductivity levels in the melt. This confirms that the four curves that are not from Knacke and Strese[54] are more reliable. The trend line that represents the system the best is that from Chun-Peng *et al.*[50] and is written as:

$$\log\left(\sigma_{Cu_2S}\right) = 4.744 - \frac{4447}{T} \qquad [36]$$
$$1420\ \mathrm{K} < T < 1590\ \mathrm{K}$$

where the conductivity is $\Omega^{-1}cm^{-1}$. This equation is a linear representation of the dependence of the electrical conductivity on temperature for molten Cu_2S. An average deviation of about 25% may be expected. From the magnitude and the temperature dependence of the electrical conductivity of Cu_2S, it is reasonable to conclude that molten Cu_2S is semiconductive.

It was stated in Knacke and Strese[47] that electrical conductivity measurements of Cu_2S can be expressed with the Arrhenius equation:

$$\log(\sigma') = B - \frac{A}{4.575 \cdot T} \qquad [37]$$

Where;

A = activation energy of the electrical conductivity (cal/mol)

T = absolute temperature, K

This equation is theoretically applicable for ion conductors and semi-conductors, and has often been used for solid materials[47]. The form of Equation [37] will therefore be used throughout this section to describe conductivity-temperature relationships of matte melts. The parameters A and B will be regressed and the conductivity will be expressed in $\Omega^{-1}cm^{-1}$.

The electrical conductivity of pure FeS at different temperatures and sulphur compositions is shown in Figure 18. The electrical conductivity of the Fe-S dropped rapidly as the sulphur content increased to a stoichiometric amount of 36.5 weight %. It is apparent that the electrical conductivity increased sharply for a slight increase in sulphur content above the stoichiometric sulphur concentration. The conductance of the Fe-S system is therefore very sensitive to the addition or contamination of sulphur.

From Figure 18 it can be seen that conductance levels from Dobrovinskii *et al.*[56], Pound *et al.*[49] and Savelsberg[46] are about three times the magnitude of those from Argyriades

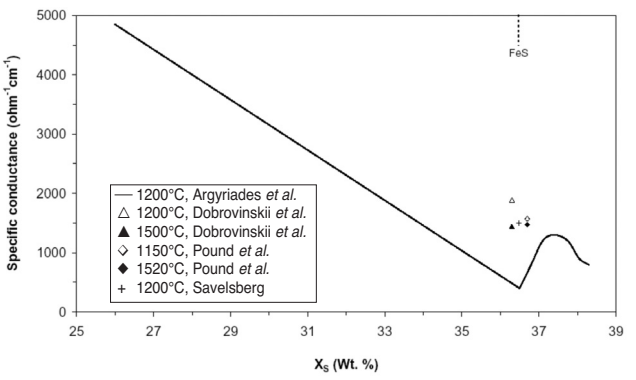

Figure 18—Plot of electrical conductivity of molten Fe-S vs. sulphur content

et al.[51]. The most probable reason for the difference between the results from Argyriades *et al.*[51] and the rest is an imbalance of sulphur in the pure FeS samples due to desulphurization during experimentation and errors during sample analyses. A local maximum for conductivity can also be seen at a sulphur concentration of 37.4%.

The sulphur content in the FeS specimens of Pound *et al.*[49] was actually less than what is indicated in Figure 18 due to desulphurization and the uncertainties involved with sulphur analysis. Modern-day techniques for sulphur analysis are much more reliable than the chemistry tests used by Pound *et al.*[49] The results from Argyriades *et al.*[51] were measured under a sulphur-controlled atmosphere. This maintains the sulphur content in the melt and prevents desulphurization. It is therefore reasonable to assume that the data from Argyriades *et al.*[51] are representative of the electrical conductivity of pure FeS.

In Figure 19, the conductivity of stoichiometric FeS tended to decrease as the temperature of the melt increased. The results from both literature sources in Figure 19 confirm that the conductivity of FeS has a negative temperature coefficient. FeS thus seems to follow the rule of thumb for metallic conductors described earlier, as it is indeed a metallic conductor according to Enderby and Barnes[53]. The accuracy of the results from Pound *et al.*[49] are not guaranteed due to imbalances and uncertainties in their analyses for sulphur. It is unknown how reliable the results from Dobrovinskii *et al.*[56] are. The best approach to quantify the temperature dependence of the conductivity for pure and sulphur deficient FeS would be to assume that an acceptable trend (see Curve A) lies between that of the two trend lines in Figure 19:

$$\log(\sigma_{FeS}) = 2.818 + \frac{618}{T} \qquad [38]$$
$$1420\ \text{K} < T < 1800\ \text{K}$$

This equation may be in error by about 10%.

The dependence of binary mixtures of pure Cu_2S and FeS on temperature change is illustrated in Figure 20, according to Pound *et al.*[49]. The binary mixture of Cu_2S and FeS follows a roughly additive rule of mixtures, as can be seen in Figure 20[51].

The negative temperature coefficient and the greater conductivity of pure FeS (about 10 times that of Cu_2S) indicates metallic conduction in FeS. The temperature coefficient remained positive in the Cu_2S-rich binary system for Cu_2S concentrations between 50 and 100 wt. %, and was negative for high concentrations of FeS that surpassed 80%. Conductivity measurements remained constant for FeS-rich systems where FeS concentrations ranged between 50 and 80%. Pound *et al.*[49] state that each conductivity-temperature relationship given in Figure 20 has an average tolerance of about 5%.

Figure 21 confirms that the Cu_2S-rich binary systems of Cu_2S-FeS have a positive temperature coefficient. An elemental composition of 40 wt. % Cu, 31.8% Fe, and 28.3% S is equivalent to a mixture of 50% Cu_2S and 50% FeS. An elemental content of 51.9% Cu, 22.2% Fe, and 25.9% S is equivalent to a binary mixture of 65% Cu_2S and 35% FeS. It is apparent from Figure 21 that their is poor agreement between the results of Chun-Peng *et al.*[50] and the others, the reason for this is not known.

The electrical conductivity of the Ni-S system is shown to decrease almost linearly with increasing temperature in Figure 22, as from Argyriades *et al.*[51]. This figure also illustrates how conductivity reaches a minimum value at the sulphur composition of stoichiometric Ni_3S_2 (26.7%).

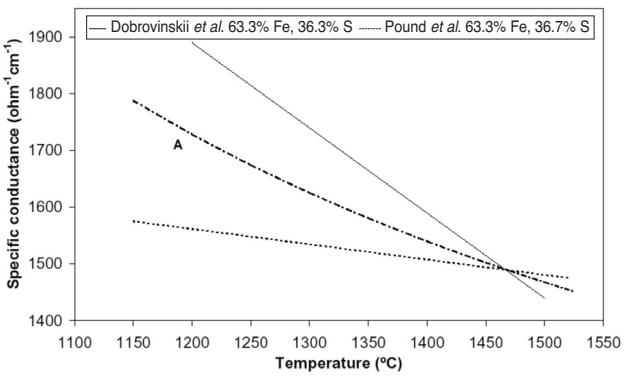

Figure 19—Conductivity-temperature relationship for stoichiometric FeS

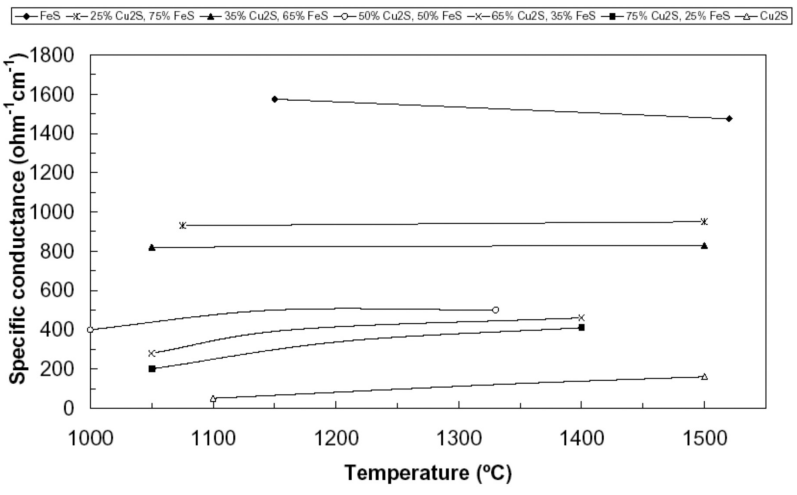

Figure 20—Summary of specific conductance data for molten mattes. Composition in wt.%[49]

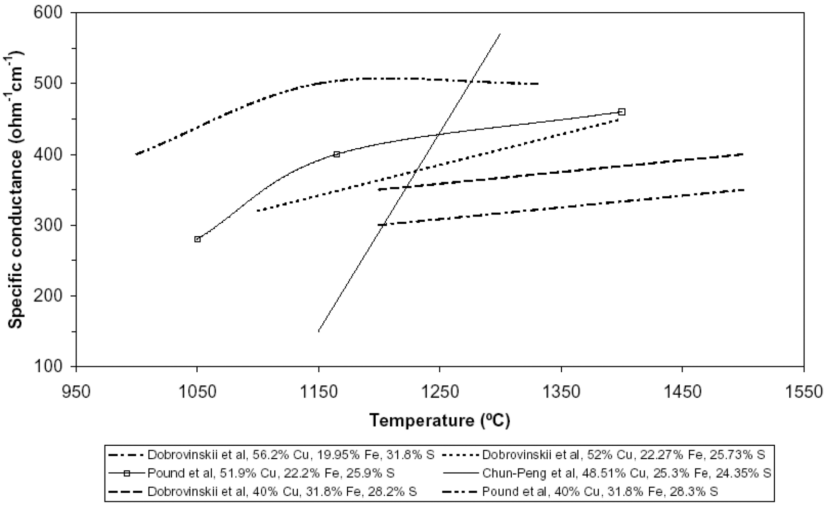

Figure 21—Conductivity of molten Cu-Fe-S at various temperatures

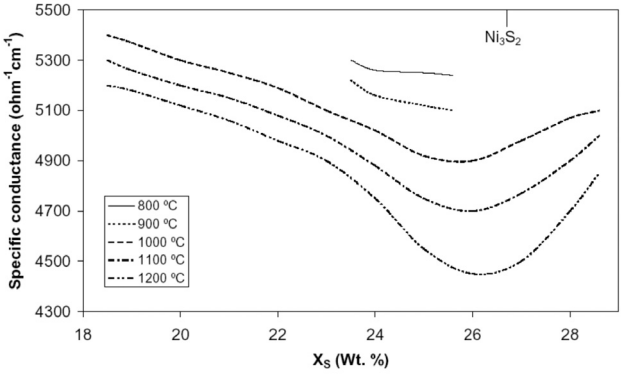

Figure 22—Dependence of the electrical conductivity of molten Ni-S on temperature and sulphur concentration[52]

The temperature dependence of the conductivity of Ni-S systems, with compositions near to stoichiometric Ni_3S_2, is displayed in Figure 23. Measurements of Curves 1, 2 and 3 in Figure 23 agree very well. The composition of the samples of these three curves lies very close to that of pure Ni_3S_2. The temperature-conductivity relationship was subsequently determined from Curves 1, 2 and 3:

$$\log\left(\sigma_{Ni_3S_2}\right) = 3.283 + \frac{537}{T} \qquad [39]$$
$$1273\ \text{K} < T < 1773\ \text{K}$$

The sulphur-rich Ni_3S_2 from Delimarskii and Belikanov[48] has a gradient that is very similar to those of Curves 1, 2 and 3, but lies more to the left at a lower temperature due to the higher concentration of sulphur. The magnitude of the conductance of pure Ni_3S_2 is roughly three times that of FeS and the negative temperature coefficient of Ni_3S_2 indicates metallic conductivity. NiS is confirmed as a metallic conductor by Enderby and Barnes[45], and this seems to hold true for Ni_3S_2.

Unusual behaviour is observed for the binary mixture of Cu_2S and Ni_3S_2 as can be seen in Figure 24 from Chun-Peng *et al.*[50]. The line shown in this Figure is valid for a temperature range from 1200 to 1400°C as Chun-Peng found that temperature had no effect on this system over this range. The system rapidly increases in conductivity as the Ni_3S_2 content increases from 40 to 90 wt.% and then suddenly drops for Ni_3S_2 concentrations that are higher than 90%. Addition of Cu_2S up to 10% seems to boost the binary

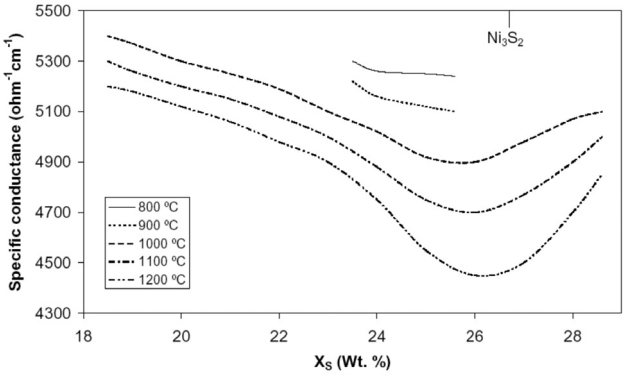

Figure 23—Decrease of electrical conductivity of Ni_3S_2 for increasing temperatures

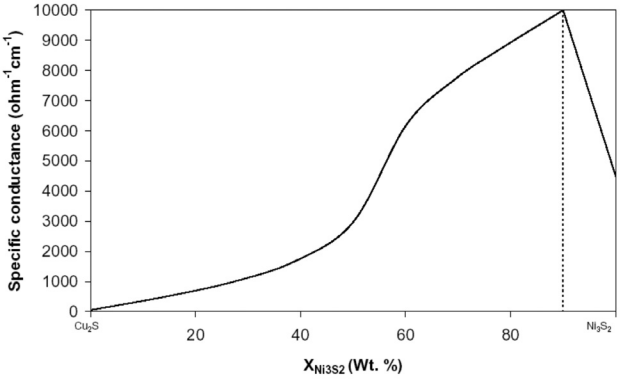

Figure 24—Conductivity data for the Cu_2S-Ni_3S_2 binary system valid for 1200–1400°C[50]

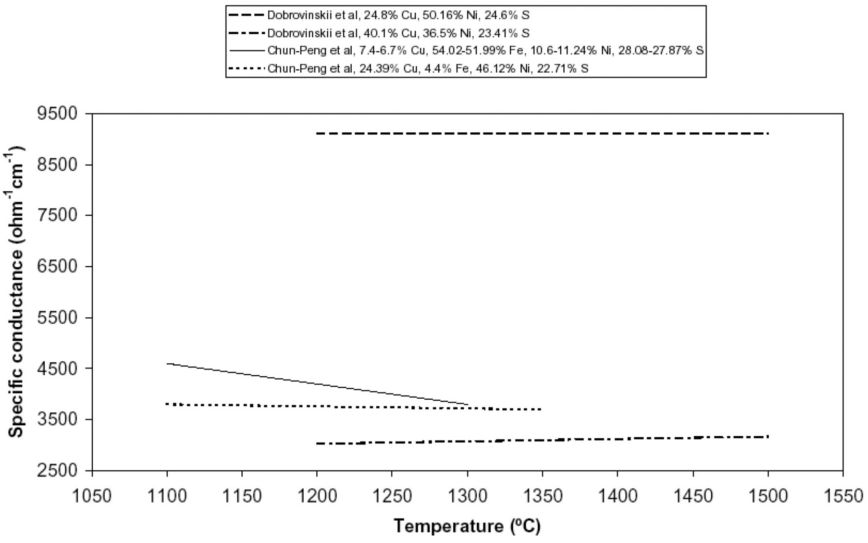

Figure 25—Illustration of conductivity measurements for combinations of Cu, Fe, Ni and S[50]

conductivity tremendously. Further additions of Cu_2S will have the effect of suppressing electrical conductivity. From 0 to 60% Ni_3S_2, conductivity increases linearly by about 400 $\Omega^{-1}cm^{-1}$ for a temperature increase from 1200 to 1400°C. Close to pure Ni_3S_2, conductivity decreases linearly by about 600 $\Omega^{-1}cm^{-1}$ for a temperature increase from 1200 to 1400°C.

In Figure 25 the electrical conductivity for mixtures of the four elements, Cu, Fe, Ni and S, in different proportions, showed similar results to what is observed in Figure 24. High concentrations of Ni in a Cu-Ni-S system bring about high conductance measurements, and subsequent additions of Cu and/or Fe tends to dilute or suppress high electrical conductance. The conductance measurements appear to remain constant across the temperature range shown in Figure 25, except for the Fe-rich system, which has a negative temperature coefficient.

The cobalt sulphide system from Dancy and Derge[52] shows electrical conductivity measurements as a function of sulphur content and temperature (see Figure 26).

Electrical conductivities of miscellaneous sulphides are illustrated as linear functions of temperature in Figure 27. Also included in this Figure is the conductivity of a typical slag encountered in PGM smelting[57]. The necessary information for the sulphides in Figure 27 was obtained from Delimarskii and Belikanov[48]. The measurements for Sb_2S_3 agreed well with the data for the same system from Knacke and Strese[47], and the data for the Ni-S system also compared reasonably well with corresponding data from Chun-Peng *et al.*[50]. It is clear that the conductivity of the slag is much lower than that of the sulphides reviewed in this section, with a conductivity between 0.15 and 0. 40 $\Omega^{-1}cm^{-1}$ in the temperature range 1350–1600°C.

Summary

Too little data are available on the subject of the thermal conductivity of liquid base metal mattes in order to make a reasonable study of it. In general, too little work has been done by researchers on quantifying the physical properties of base metal mattes and particular attention needs to be focused on determining the properties of multi-component matte systems for which literature is scarce. An abundance of information exists for slag systems primarily because of the necessary heat that is generated when current is passed through it. Many other influences of slag also make it a very

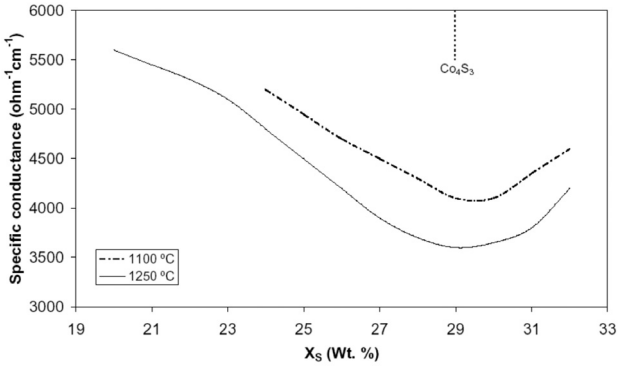

Figure 26—Measurements of the electrical conductivity of Co-S[52]

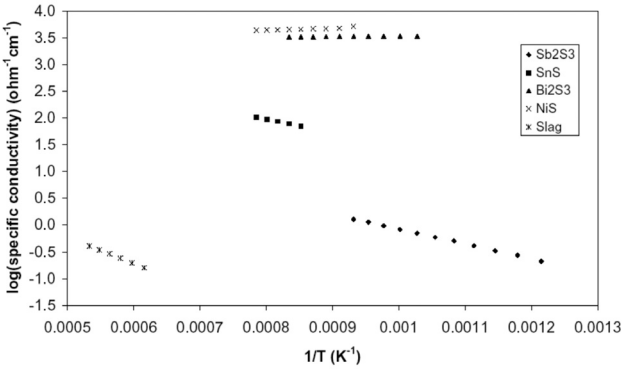

Figure 27—Summary of the electrical conductance of Sb_2S_3, SnS, Bi_2S_3, NiS[48] and a slag of composition (wt.%) 15% FeO, 5% Al_2O_3, 20% MgO, 10% CaO, and 50% SiO_2[57]

important aspect of furnace operation. The characteristics of matte systems are important when studying the separability of matte from slag in smelting operations. Matte properties also affect the dynamics of converter furnaces, which are designed to reduce the sulphur content of molten matte by means of gas blowing. A greater understanding of the properties of matte systems may lead to the improvement of many matte treatment processes and may also open doors to the development of new technologies for the treatment of matte. To conclude the work in this review, a summary of all the main findings are provided with reference to the equations and figures in the text.

Viscosity

Figure 1 can be used to estimate the viscosity of pure matte compounds Ni_3S_2, FeS, and Cu_2S at temperatures ranging from about 1000 K to 1600 K. Viscosity values for each compound decreased with temperature, while that of FeS increased unexpectedly as a probable result of complex formation within the structural units of FeS. Viscosity values for mattes with compositions near that of the pseudo-binary systems Cu_2S-Ni_3S_2, FeS-Cu_2S, FeS-Ni_3S_2, FeS-Co_4S_3, and Ni_3S_2-Co_4S_3 are given in Figure 2 and Figure 3. Measurements in some of these figures demonstrated anomalous behaviour below temperatures of 1250°C. Viscosity behaviour above 1250°C appears to be normal and it may be assumed that measurements have an average error of about 10%.

Density

Equation [2] can be used to quantify the density of Cu-Ni-Fe-S mattes as a function of elemental matte composition and temperature. A maximum error of about 5% may occur if the equation is used within the specified compositional ranges. Density values of molten mattes are fairly insensitive to changes in temperature. A density decrease of about 0.2 g/cm3 may result if the temperature is raised by 100°C. Linear regression models for the pure compounds Ni_3S_2, Cu_2S, and FeS are given in Equations [3] to [5] and are applicable for temperatures up to 1300°C. Equations [6] to [8] relate the densities of pseudo-binary systems of Ni-Cu-Fe-S mattes to compositional change at a fixed temperature of 1200°C. Equation [6] is a third order polynomial for calculating the density of FeS-Ni_3S_2 matte and may have an error of about 5%. Equation [7] is a linear model for determining the density of Cu_2S-Ni_3S_2 matte and may have a maximum error of 10%. Equation [8] is applicable to the Cu_2S-FeS system. It is also linear and may have an error of 10%.

Figure 5 is a pseudo-ternary diagram of Ni_3S_2-Cu_2S-FeS mattes at 1200°C. From this diagram it is evident that Cu_2S addition to the matte has a weak effect on matte density. Density readings appear to be more sensitive when the FeS concentration is high within the system.

Surface tension

The temperature dependence of surface tension measurements for pure Ni_3S_2, Cu_2S, and FeS is illustrated in Figure 6. Cu_2S and FeS show negligible temperature dependency and the surface tension of Ni_3S_2 decreases linearly with increasing temperature. Equations [12] and [13] are reliable expressions for calculating the surface tensions of Ni-Fe-S and Ni-Cu-Fe matte mixtures respectively at 1200°C. The only input criteria for these equations are elemental compositions. Appropriate models for calculating surface tensions of the Ni-Cu-Fe-S pseudo-binaries were derived by regressing the experimental results of various investigators (Equations [16] to [18]). These equations may have an average error of about 10%. A linear relationship was found to exist between the Ni_3S_2 concentration and the contact angle of Ni-Fe-S matte on different substrates (see Equations [19] to [23]). The contact angle increases with increasing nickel sulphide content in the matte regardless of the type of substrate used. Silica was found to be far less wettable than the other substrates. The Ni_3S_2-Cu_2S-FeS pseudo-ternary diagram (Figure 12) of surface tensions at 1200°C shows that Cu_2S addition to the system does not reduce the surface tension significantly. Surface tension values are, however, sensitive to compositional changes at high concentrations of Ni_3S_2. The surface tension data shown in Figure 12 was fit using a cubic polynomial (Equation [26]), the error from the fit was below the experimental error of the data.

Interfacial tension

Interfacial tension between Ni-Fe-S matte and fayalite slag is well represented by Equations [31] and [32] for an average Fe/SiO_2 (wt/wt) ratio of about 1.6. The interfacial tension of this system also increases almost linearly from 0.02 to 0.1 N/m when the copper grade is increased from 0 to 80%.

Electrical conductivity

Figure 16 may be used to determine the electrical conductivity of Cu-S systems at different concentrations of sulphur. Copper-rich Cu_2S matte maintains a constant electrical conductivity according to Equation [34] and has an accuracy of about 20%. The conductance of sulphur-rich Cu_2S matte increases exponentially according to Equation [35] and may deviate by 50% or more.

The conductivity of Cu_2S matte has a positive temperature dependence, meaning that electrical conductivity increases with temperature. This can be seen in Figure 17, and the conductivity of Cu_2S can be calculated according to Equation [36] which may be in error by 25%. From the magnitude and the temperature dependence of the electrical conductance of Cu_2S, it was concluded that molten Cu_2S behaves as a semiconductor. The conductivity of pure FeS at different temperatures and sulphur compositions is illustrated in Figure 18. The conductivity drops rapidly as the sulphur content increases to the stoichiometric sulphur content of pure FeS, and it increases for a slight increase in sulphur content. The cluster of measurements above the solid line in Figure 18 may be slightly inaccurate due to desulphurization during experimentation and errors during sample analyses. The results from Argyriades *et al.*[51] were assumed to be the most accurate due to improved experimental conditions. The dependence of the electrical conductance of FeS on temperature may be determined with Equation [38]. The results may be in error by about 10%. A binary mixture of

Cu_2S and FeS follows a roughly additive rule of mixtures as can be seen in Figure 20. The negative temperature coefficient and the greater conductivity of FeS indicates metallic conductance in FeS. The temperature coefficient of the binary concentration of FeS exceeds 80%. Figure 22 shows that the Ni-S system also has a minimum conductivity at the stoichiometric composition of Ni_3S_2. The conductivity-temperature relationship is well defined with Equation [39]. The negative temperature coefficient and the greater conductance levels for Ni-S systems indicate metallic conductivity.

Binary mixtures of Cu_2S and Ni_3S_2 do not follow an additive rule as for the FeS-Cu_2S systems, but show anomalous behaviour at high Ni_3S_2 concentrations as can be seen in Figure 24. Similar behaviour exists in Figure 25, where high concentrations of Ni in the Ni-Cu-S system bring about elevated conductance measurements. Subsequent additions of Cu and/or Fe tend to dilute or suppress high electrical conductance. Conductivity levels remain fairly constant in the Cu-Ni-S system over a wide range of temperatures and metal-compositions. Additions of small amounts of Fe to this system (<10%) have a negligible effect on the temperature gradient. Higher concentrations of Fe do, however, cause the temperature coefficient to become negative as for pure FeS.

Conductivity data may be determined for the Co-S system from the data illustrated in Figure 26. Figure 27 shows the temperature-composition relationship for additional sulphide systems of Sb_2S_3, SnS, Bi_2S_3 and NiS as well as a typical slag as is encountered in the smelting of PGMs.

Acknowledgements

The authors would like to express their appreciation towards the following persons, all chemical engineers, who aided in the translation of many of the references:

- Mr. Tafirenyika Madzimbamuto, from the Cape Peninsula University of Technology, for translation of journal papers from Russian
- Dr. Cara Schwartz, from Stellenbosch University, for translation of journal papers from German
- And Mr. Qian Wang, from Stellenbosch University, for translation of journal papers from Chinese.

The financial support of the South African National Research Foundation is acknowledged with appreciation.

References

1. Nikiforov, L.V., Nagiev, V.A., and Grabchak, V.P. Viscosity of sulphide melts. Izvestiya Akademii Nauk SSSR, *Neorganicheskie Materialy*, vol. 12, no. 7, 1976. pp. 1179–1182.
2. Glazov, V.M., Chizhevskaya, S.M., and Glagoleva, N.N. *Liquid semiconductors* (in Russian). Nauka, 1967.
3. Dobrovinskii, I.E., Esin, O.A., Bormin, L.N., and Chuchmarev, S.K. Variation of the volume and viscosity of sulphide melts with composition. *Russian Journal of Inorganic Chemistry*, vol. 14, no. 5, 1969. pp. 727–730.
4. Barfield, R.N. and Kitchener, J.A. The viscosity of liquid iron and iron-carbon alloys. *Journal of the Iron and Steel Institute*, vol. 180, 1955. pp. 324–329.
5. Kucharski, M., Ip, S.W., and Toguri, J.M. The surface tension and density of Cu_2S, FeS, Ni_3S_2 and their mixtures. *Canadian Metallurgical Quarterly*, vol. 33, no. 3, 1994. pp. 197–203.
6. Kongoli, F., Dessureault, Y., and Pelton, A.D. Thermodynamic modeling of liquid Fe-Ni-Cu-Co-S mattes. *Metallurgical and Materials Transactions B*, vol. 29, 1998. pp. B:591–601.
7. Waldner, P. and Pelton, A.D. Critical thermodynamic assessment and modelling of the Fe-Ni-S system. *Metallurgical and Materials Transactions B*, vol. 35B, 2004. pp. 897–907.
8. Kongoli, F. and Pelton, A.D. Model prediction of thermodynamic properties of Co-Fe-Ni-S mattes. *Metallurgical and Materials Transactions B*, vol. 30B, 1999. pp. 443–450.
9. Pelton, A.D. and Blander, M. Thermodynamic analysis of ordered liquid solutions by a modified quasichemical approach-application to silicate slags. *Metallurgical and Materials Transactions B*, vol. 17B, 1986. pp. 805–815.
10. Eriksson, G. and Pelton, A.D. Critical evaluation and optimization of the thermodynamic properties and phase diagrams of the calcia-alumina, alumina-silica, and calcia-alumina-silica systems. *Metallurgical and Materials Transactions B*, vol. 24B, 1993. pp. 807–816.
11. Wu, P., Eriksson, G., and Pelton, A.D. Critical evaluation and optimization of the thermodynamic properties and phase diagrams of the calcia-iron(II) oxide, calcia-magnesia, calcia-manganese(II) oxide, iron(II) oxide-magnesia, iron(II) oxide-manganese(II) oxide, and magnesia-manganese(II) oxide systems. *Journal of the American Ceramic Society*, vol. 76, 1993. pp. 2059–2064.
12. Kondratiev, A., Hayes, P.C. and Jak, E. Development of a quasi-chemical viscosity model for fully liquid slags in the Al_2O_3-CaO-FeO-MgO-SiO_2 system.Part 1. Description of the model and its application to the MgO, MgO-SiO_2, Al_2O_3-MgO and CaO-MgO sub-systems. *ISIJ International*, vol. 45, no. 3, 2006. pp. 359–367.
13. Friedrich, K. Investigation of layer-forming systems. *Metall und Erz*, 1914. pp. 160–167.
14. Levin, E.M., Robbins, C.R., and McMurdie, H.F. Phase diagrams for ceramists. *The American Ceramic Society*, 1964.
15. Glazov, V.M. and Vertman, A.A. *The structure and properties of liquid metals* (in Russian). Izd-vo AN SSSR, 1960.
16. Larrain, J.M. and Lee, S.L. Thermodynamic properties of copper-nickel-sulfur melts. *Canadian Metallurgical Quarterly*, vol. 19, 1980. pp. 183–190.
17. Lee, S.L., Larrain, J.M., and Kellogg, H.H. Thermodynamic properties of molten sulphides. Part III. The system Cu-Ni-S. *Metallurgical Transactions B*, vol. 11B, 1980. pp. 251–255.
18. Kopylov, N.I. and Novoselov, S.S. System Cu_2S-FeS-Na_2S. *Zhurnal Neorganicheskoi Khimii*, vol. 9, no. 8, 1964. pp. 1919–1929.
19. Kaiura, G.H. and Toguri, J.M. Densities of the molten ferrous sulfide, ferrous sulfide-cuprous sulfide and iron-sulfur-oxygen systems—utilizing a bottom-balance Archimedean technique. *Canadian Metallurgical Quarterly*, vol. 18, no. 2, 1979. pp. 155–164.
20. Nagamori, M. Density of molten silver-sulfur, copper-sulfur, iron-sulfur, and nickel-sulfur systems. *Transactions of the American Institute of Mining, Metallurgical and Petroleum Engineers,* vol. 245, no. 9, 1969. pp. 1897–1902.
21. Fujisawa, T. Utigard, T., and Toguri, J.M. Surface tension and density of the molten lead chloride-potassium chloride-sodium chloride ternary system. *Canadian Journal of Chemistry*, vol. 63, no. 5, 1985. pp. 1132–1138.
22. Liu, G., Toguri, J.M., and Stubina, N.M. Surface tension and density of the molten $LaCl_3$-NaCl binary system. *Canadian Journal of Chemistry*, vol. 65, no. 12, 1987. pp. 2779–82.
23. Byerley, J.J. and Takebe, N. Densities of molten nickel mattes. *Metallurgical Transactions*, vol. 2, no. 4, 1971. pp. 1107–1111.
24. Azuma, K. and Takebe, N. Densities of molten copper matte. *Nippon Kogyo Kaishi*, vol. 88, 1972. pp. 557–562.
25. Tokumoto, S., Kasama, A., and Fujioka, Y. Measurements of density and surface tension of copper mattes. *Technology Reports of the Osaka University*, 22, 1972. pp. 1053–1089.
26. Hyrn, J.N., Toguri, J.M., Choo, R.T.C., and Stubina, N.M. Densities of molten copper-nickel mattes between 1100 and 1300°C. *Canadian Metallurgical Quarterly*, vol. 35, no. 2, 1996. pp. 123–132.
27. Ip, S.W. and Toguri, J.M. Surface and interfacial tension of the Ni-Fe-S, Ni-Cu-S, and fayalite slag systems. *Metallurgical Transactions B*, vol. 24, 1993. pp. 657–668.

28. Matsushita, T., Hayashi, M., and Seetharaman, S. Thermochemical and thermophysical property measurements in slag systems. *International Journal of Materials and Product Technology*, vol. 22, no. 4, 2005. pp. 351–390.

29. Mandira, M., Dharwadkar, H.N., and Kumar, D. Surface tension of matte and its measurement by sessile drop technique. *Transactions of the Institution of Mining and Metallurgy, Section C: Mineral Processing and Extractive Metallurgy*, vol. 96, June 1987. pp. C93–C97.

30. Halden, F.A., and Kingery, W.D. Surface tension at elevated temperatures. II. Effect of C, N, O and S on liquid iron surface tension and interfacial energy with Al_2O_3. *Journal of Physical Chemistry*, vol. 59, 1955. pp. 557–559.

31. Nakashima, K. and Mori, K. Interfacial properties of liquid iron alloys and liquid slags relating to iron- and steel-making processes. *ISIJ International*, vol. 32, 1992. pp. 11–18.

32. GaleW.F. and Totemeier, T.C. (eds). *Smithells metals reference book.* Elsevier Butterworth-Heinemann, Oxford, England, 8th edition, 2004.

33. Hengzhong, Z. Relationship between the surface tensions and the compositions of copper and nickel mattes. *Paul E. Queneau International Symposium on Extractive Metallurgy of Copper Nickel and Cobalt*, vol. 1, 1993. pp. 341–351.

34. Krivsky, W.A. and Schuhmann, R. Thermodynamics of the Cu-Fe-S system at matte smelting temperatures. *Transactions of the American Institute of Mining and Metallurgy*, vol. 209, 1957. pp. 981–988.

35. Elliott, J.F. and Mounier, M. Surface and interfacial tensions in copper matte-slag systems, 1200°C. *Canadian Metallurgical Quarterly*, vol. 21, no. 4, 1982. pp. 415–428.

36. Vanyukov, A.V., Bystrov, V.P., and Ya, V. Zaitsev. Surface and interfacial tension of lead-bearing metallurgical melts. *Eizicheskaya Khimiya Metallurgicheskih Protsessov I Sistem*, 1966. pp. 396–406.

37. Yan, L., Cao, Z., Xie, Y., and Qiao, Z. Surface tension calculation of the Ni_3S_2-FeS-Cu2S mattes. *Calphad*, vol. 24, no. 4, 2000. pp. 449–463.

38. Hillert, M. Empirical methods of predicting and representing thermodynamic properties of ternary solution phases. *Calphad*, vol. 4, no. 1, 1980. pp. 1–12.

39. Chou, K.-C., Li, W.-C., Li, F., and He, M. Formalism of new ternary model expressed in terms of binary regular-solution type parameters. *Calphad*, vol. 20, no. 4, 1996. pp. 395–406.

40. Girifalco, L.A. and Good, R.J. A theory for the estimation of surface and interfacial energies. I. Derivation and application to interfacial tension. *Journal of Physical Chemistry*, vol. 61, 1957, pp. 904–909.

41. Ya. Zaitsev, V., Vanyukov, A.V., and Kolosova, V.S. Interaction of Ni_3S_2-FeS and Cu_2S-FeS sulfide systems with iron-silicate melts. *Izvestiya Akademii Nauk SSSR, Metally*, vol. 5, 1968. pp. 39–45.

42. Mungall, J.E. and Su, S. Interfacial tension between magmatic sulfide and silicate liquids: Constraints on kinetics of sulfide liquation and sulfide migration through silicate rocks. *Earth and Planetary Science Letters*, vol. 234, 2005. pp. 135–149.

43. Urquhart, R.C., Rennie, M.S., and Rabey, C.C. *Extractive metallurgy of copper, pyrometallurgy and electrolytic refining*, chapter 14: The smelting of copper-nickel concentrates in an electric furnace, Metallurgical Society of the AIME, 1976. pp. 274–295.

44. Hayes, P. *Process principles in minerals and materials production*. Hayes Publishing Co., 3rd edition, 2003.

45. Enderby, J.E. and Barnes, A.C. Liquid semiconductors. *Reports on Progress in Physics*, vol. 53, 1990. pp. 85–179.

46. Savelsberg, W. Ueber die elektrolyse geschmolzener metallsulfide. *Zeitschrift fuer Elekrochemie und Angewandte Physikalische Chemie*, vol. 46, no. 7, 1940. pp. 379–397.

47. Knacke, O. and Strese, G. Die elektrische leitfähigkeit von geschmolzenen sulfiden, schlacken und speisen. *Zeitschrift fuer Erzbergbau und Metallhuettenwesen*, vol. 10, no. 5, 1957, pp. 207–212.

48. Delimarskii, Y.K. and Belikanov, A.A. The electrical conductivity of molten sulphides of tin, antimony, bismuth and nickel. *Journal of Inorganic Chemistry*, vol. 111, no. 5, 1958. pp. 1075–1078.

49. Pound, G.M., Derge, G., and Osuch, G. Electrical conduction in molten Cu-Fe sulphide mattes. *Journal of metals*, vol. 7, no. 3, 1955. pp. 481–484.

50. Chun-Peng, L., Ming-Shi, C., and Ai-Ping, H. Specific conductance of copper(I) sulfide, nickel(II) sulfide and commercial mattes. *Youse Jinshu*, vol. 32, no. 1, 1980. pp. 76–81.

51. Argyriades, D., Derge, G., and Pound, G.M. Electrical conductivity of molten FeS. *Transactions of the Metallurgical Society of AIME*, vol. 215, no. 6, 1959. pp. 909–912.

52. Dancy, E.A. and Derge, G.J. Electrical conductivity of the molten Co-S, Ni-S, Cu-S, and Ag-S systems. *Transactions of the Metallurgical Society of AIME,* vol. 227, no. 5, 1963. pp. 1034–1038.

53. Enderby, J.E. and Barnes, A.C. A theory for the electrical conductivity of molten mixtures of sulphides and halides. *Journal of the Electrochemical Society*, vol. 134, no. 10, 1987. pp. 2483–2485.

54. Bourgon, M., Derge, G., and Pound, G.M. Conductivity and sulfur activity in liquid copper sulfide. *Journal of metals*, vol. 9, no. 11, 1957. pp. 1454–1458.

55. Yang, L., Pound, G.M., and Derge, G. Mechanism of electrical conduction in molten Cu_2S-CuCl and mattes. *Transactions of the Metallurgical Society of AIME*, vol. 206, no. 5, 1956, pp. 783–788.

56. Dobrovinskii, I.E., Esin, O.A., and Barmin, L.N. Electroresistance of melts containing iron, nickel, cobalt, and copper sulphides. Izvestiya Vysshikh Uchebnykh Zavedenii, *Tsvetnaya Metallurgiya*, vol. 13, no. 2, 1970. pp. 73.

57. Hundermark, R. The electrical conductivity of melter type slags. Master's thesis, University of Cape Town, 2003. ◆

Erratum

Paper entitled: 'Comparative study of the influence of minerals in gas sorption isotherms of three coals of similar rank', by C. Rodrigues, H.J. Pinheiro, M. J. Lemos de Sousa, published in the *Journal* of The Southern African Institute of Mining and Metallurgy, vol. 108, no. 7, pp. 371–375. July 2008.

The following are the correct legends for Figures 4 to 7:

Figure 4—Sample A: comparison between isotherm of the raw coal with calculated weighted isotherm using float and sink sorption data.
Figure 5—Sample B: comparison between isotherm of the raw coal with calculated weighted isotherm using float and sink sorption data.
Figure 6—Sample C: comparison between isotherm of the raw coal with calculated weighted isotherm using float and sink sorption data.
Figure 7—Relation between maximum adsorption and ash per cent (dry basis).